GEOTRACES Intercalibration of the Stable Silicon Isotope Composition of Dissolved Silicic Acid in Seawater

Author(s):
Grasse, Patricia; Brzezinski, Mark A.; De Souza, Gregory F.; Andersson, Per; Closset, Ivia; Cao, Zhimian; Dai, Minhan; Ehlert, Claudia; Estrade, Nicolas; François, Roger; Frank, Martin; Jiang, Guibin; Jones, Janice L.; Kooijman, Ellen; Liu, Qian; Lu, Dawei; Ponzevera, Emanuel; Schmitt, Melanie; Sun, Xiaole; Sutton, Jill N.; Thil, François; Weis, Dominique; Wetzel, Florian; Zhang, Anyu; Zhang, Jing; Zhang, Zhouling

Publication date:
2017-03

Permanent link:
https://doi.org/10.3929/ethz-b-000127180

Originally published in:
Journal of Analytical Atomic Spectrometry 32(3), https://doi.org/10.1039/C6JA00302H

GEOTRACES Intercalibration of the Stable Silicon Isotope Composition of Dissolved Silicic Acid in Seawater

Patricia Grasse[1,2,17], Mark A. Brzezinski[2,16], Damien Cardinal[3], Gregory F. de Souza[4], Per Andersson[5], Ivia Closset[3], Zhimian Cao[6], Minhan Dai[6], Claudia Ehlert[7], Nicolas Estrade[8,9], Roger François[8], Martin Frank[1], Guibin Jiang[10], Janice L. Jones[2], Ellen Kooijman[5], Qian Liu[10], Dawei Lu[10], Katharina Pahnke[7], Emanuel Ponzevera[11], Melanie Schmitt[5], Xiaole Sun[12], Jill N. Sutton[13], François Thil[14], Dominique Weis[8], Florian Wetzel[4], Anyu Zhang[15], Jing Zhang[6], Zhouling Zhang[6]

[1]GEOMAR
Helmholtz Centre for Ocean Research Kiel
Ocean Circulation and Climate Dynamics
Wischhofstr. 1-3
24148 Kiel,
Germany

[2]Marine Science Institute and the Department of Ecology, Evolution, and Marine Biology &
University of California,
Santa Barbara, CA 93106
USA

[3]Sorbonne Universités (UPMC, Univ Paris 06)-CNRS-IRD-MNHN,
LOCEAN Laboratory,
4 place Jussieu, F-75005 Paris,
France

[4]ETH Zurich, Institute of Geochemistry and Petrology
Clausiusstrasse 25
8092 Zürich,
Switzerland

[5]Swedish Museum of Natural History
Department of Geosciences
104 05 Stockholm,
Sweden

[6]State Key Laboratory of Marine Environmental Science,
Xiamen University,
Xiamen,
China

[7]Max Planck Research Group for Marine Isotope Geochemistry
Institute for Chemistry and Biology of the Marine Environment (ICBM)
University of Oldenburg
Carl-von-Ossietzky-Str. 9-11,

26129 Oldenburg,
Germany

[8]University of British Columbia
Pacific Center for Isotopic and Geochemical Research
Department of Earth, Ocean and Atmospheric Sciences
Vancouver, British Columbia,
Canada V6T 1Z4

[9]present address: LEGOS, Equipe TIM
Observatoire Midi Pyrénées; 14 av Edouard Belin; 31400
Toulouse,
France

[10]State Key Laboratory of Environmental Chemistry & Ecotoxicology
Research Center for Eco-Environmental Sciences, Chinese Academy of Sciences
18 Shuangqing Road, Haidian District, Beijing 100085,
China

[11] Unité de Recherche Géosciences Marines, IFREMER,
29870, Plouzané,
France

[12]Department of Environmental Science and Analytical Chemistry
Stockholm University
Stockholm,
Sweden
Current affiliation:
Baltic Sea Center
Stockholm University
106 91 Stockholm
Sweden

[13]Université de Brest, CNRS, IRD, IFREMER, LEMAR, IUEM
Rue Dumont d'Urville, 29870, Plouzané,
France.

[14]LSCE/IPSL - Laboratoire des Sciences du Climat et de l'Environnement
Laboratoire CEA-CNRS-UVSQ
Bât 12, Domaine du CNRS, Avenue de la Terrasse
F-91198 Gif sur Yvette Cedex,
France

[15]State Key Laboratory of Estuarine and Coastal Research,
East China Normal University, Shanghai 200062,
China

[16]corresponding author

[17]second corresponding author

Abstract

The first inter-calibration study of the stable silicon isotope composition of dissolved silicic acid in seawater, $\delta^{30}Si(OH)_4$, is presented as a contribution to the international GEOTRACES program. Eleven laboratories from seven countries analyzed two seawater samples from the north Pacific subtropical gyre (Station ALOHA) collected at 300 m and at 1000 m water depth. Sampling depths were chosen to obtain samples with a relatively low (9 μmol L^{-1}, 300 m) and a relatively high (113 μmol L^{-1}, 1000 m) silicic acid concentration as sample preparation differs for low- and high- concentration samples. Data for the 1000m water sample were not normally distributed so the median is used to represent the central tendency for the two samples. Median $\delta^{30}Si(OH)_4$ values of +1.66 ‰ for the low-concentration sample and +1.25 ‰ for the high-concentration sample were obtained. Agreement among laboratories is overall considered very good; however, small but statistically significant differences among the mean isotope values obtained by different laboratories were detected likely reflecting interlaboratory differences in chemical preparation including pre-concentration and purification methods together with different volumes of seawater volume analyzed, and the use of different mass spectrometers including the Neptune MC-ICP-MS (Thermo Fisher™, Germany), the Nu Plasma MC-ICP-MS (Nu Instruments™, Wrexham, UK), and the Finnigan™ (now Thermo Fisher™, Germany) MAT 252 IRMS. Future studies analyzing $\delta^{30}Si(OH)_4$ in seawater should also analyze and report values for these same two reference waters in order to facilitate comparison of data generated among and within laboratories over time.

Introduction

The stable isotope composition of silicon in dissolved silicic acid in seawater, $\delta^{30}Si(OH)_4$, is a powerful tool for understanding the silicon cycle in the ocean as it reflects changes in the biological utilization of silicic acid, $Si(OH)_4$, by diatoms in surface water as well as water mass mixing. $\delta^{30}Si$ measurements in both $Si(OH)_4$ and in biogenic silica are essential to fully understand the marine Si cycle, in particular to characterize Si sources and sinks in order to better constrain the Si budget in the ocean (Tréguer and De La Rocha, 2013). Besides their importance in understanding the present day Si cycle, $\delta^{30}Si$ measurements are increasingly being used to assess past changes through the isotopic analysis of Si in biogenic silica within diatom frustules and within sponge spicules from marine sediments (e.g. Reynolds et al., 2008; Maier et al., 2013; Ehlert et al., 2015).

Beginning with the first report of $\delta^{30}Si$ measurements in natural waters by De La Rocha et al. (2000), there has been a growing number of publications, especially in the past five years, reporting $\delta^{30}Si(OH)_4$ values from marine systems, covering locations in the Southern, Atlantic, Pacific, and Indian Oceans as well as large estuaries (e.g. Cardinal et al., 2005; Reynolds et al., 2006; Cao et al., 2012; de Souza et al, 2012a; Brzezinski & Jones, 2015; Singh et al., 2015, Zhang et al. 2015a). This data set is anticipated to grow as part of the international GEOTRACES program that seeks to understand the global-scale distributions of trace elements and their isotopes in the marine environment (http://www.geotraces.org). All Si isotope data obtained by the GEOTRACES and other programs need to be fully comparable in order to better understand Si isotope systematics across the global ocean, and to validate models of the global marine $\delta^{30}Si(OH)_4$ distribution (de Souza et al., 2014, 2015; Holzer and Brzezinski, 2015; Gao et al., 2016). However, such efforts are challenged by the lack of seawater reference material of known $\delta^{30}Si(OH)_4$ to intercalibrate data generated by different laboratories or within a laboratory through time, as is currently only possible for solid siliceous materials (Reynolds et al., 2007).

The procedures and instrumentation used in stable Si isotope analysis have evolved substantially over the last two decades. The first precise $\delta^{30}Si$ measurements of marine dissolved and particulate Si were conducted using a VG Prism gas source isotope ratio mass spectrometer (IRMS) with samples prepared using a manual fluorination line that employed F_2 gas to convert Si recovered from either seawater or from biogenic silica as solid SiO_2 to SiF_4 gas (De La Rocha et al., 1996, 1997). IRMS methods have since been improved with SiF_4 now produced from acid

decomposition of Cs_2SiF_6 in an automated process employing a modified Kiel III carbonate device and a MAT 252 IRMS (Brzezinski et al., 2006). The first multi-collector inductively coupled plasma mass spectrometer MC-ICP-MS (Nu Plasma™, Nu Instruments, Wrexham, UK) measurements were performed by De La Rocha (2002). This method was improved by Cardinal et al. (2003), who used a dry-plasma mode and Mg doping to correct for mass bias. These early MC-ICP-MS studies measured $\delta^{29}Si$ (calculated from $^{29}Si/^{28}Si$; c.f. Eqn. 1) to avoid the polyatomic interference of $^{14}N^{16}O^+$ on *m / z* ^{30}Si, but this interference has since been overcome by the higher resolving power of new instruments, with all current studies reporting $\delta^{30}Si$ values. However, it is possible to convert between the two values using the relationship $\delta^{29}Si = 0.51 \times \delta^{30}Si$, assuming pure kinetic isotope fractionation of Si (cf. Reynolds et al., 2007). $\delta^{30}Si$ isotope measurements have now been successfully performed on a Neptune and Neptune *Plus* MC-ICP-MS (Thermo Fisher™, Germany, e.g. De La Rocha et al., 2011; Zhang et al., 2015b), various types of MC-ICP-MS produced by Nu Instruments™ (Wrexham, UK), including a Nu Plasma (e.g. Cardinal et al., 2005), Nu Plasma HR (e.g. Grasse et al., 2013), and the Nu Plasma 1700 high-resolution MC-ICP-MS (e.g. Reynolds et al., 2006), as well as on a Finnigan™ MAT 252 IRMS (e.g. Beucher et al., 2008).

Both mass spectrometry types (MC-ICP-MS and IRMS) produce reliable $\delta^{30}Si(OH)_4$ data with a long-term reproducibility of 0.1 - 0.2 ‰ (2 s. d., e.g. Cardinal et al., 2003; Brzezinski and Jones, 2015). A major advantage of MC-ICP-MS over current IRMS methods is the significantly lower sample mass (~0.2 µmol Si) required for analysis compared to current methods using IRMS that require approximately 10 times higher mass, necessitating a much larger sampling volume which may become prohibitively large for Si-depleted near-surface waters. On the other hand, IRMS measurements have fewer problems with molecular mass interferences, given that Si is measured in the form of SiF_3^+ at *m / z* 85, 86, 87. Interference from $SiOF_2$ with $^{29}Si^{18}OF_2^+$, $^{30}Si^{17}OF_2^+$ at *m / z* 85 and $^{30}Si^{18}OF_2^+$ at *m / z* 86 is possible and can be detected by the presence of the same oxyfluorides containing the far more abundant ^{16}O and ^{28}Si atoms at *m / z* 82, 83 and 84. Such interferences are rare with current sample preparation methods. With MC-ICP-MS, Si is measured as elemental Si with potential polyatomic interferences from C, H, O and N (e.g. $^{14}N_2$, $^{14}N_2{}^1H$, $^{12}C^{16}O$, $^{12}C^1H^{16}O$, $^{14}N^{16}O$) that can bias beam intensities for *m / z* ^{28}Si, ^{29}Si and ^{30}Si. Care must also be taken to eliminate matrix effects that may be caused by remnants of dissolved organic matter and anions such as sulfate (van den

Boorn et al., 2009; Hughes et al., 2011). For a detailed comparison between IRMS and MC-ICP-MS measurements see Reynolds et al. (2007).

Recent studies of $\delta^{30}Si(OH)_4$ distribution in deep waters (>1000 m) in the Atlantic Ocean by de Souza et al. (2012b) and by Brzezinski and Jones (2015) highlight the need for improved intercalibration among laboratories measuring $\delta^{30}Si(OH)_4$. $\delta^{30}Si(OH)_4$ values at these depths are expected to be invariant over the relatively short period of time separating these studies, yet comparison of $\delta^{30}Si(OH)_4$ data between these two studies showed a near constant offset of approximately 0.22 ‰ between samples of comparable silicic acid concentration (see Figure 2 in Brzezinski and Jones, 2015). Brzezinski and Jones (2015) could not explain the offset, as $\delta^{30}Si$ values for solid Si standards reported by both laboratories were in good agreement. Given that sample preparation methods for samples of solid and dissolved Si differ considerably (Georg et al., 2006, Reynolds et al. 2006) and in view of the fact that seawater represents a complex matrix of anions and cations, the use of solid standards, and especially of relatively pure siliceous materials, cannot account for sample preparation biases arising during the preparation of seawater samples, motivating the establishment of reference seawaters for this purpose.

The only inter-laboratory calibration of Si isotope standards to date was conducted with solid Si material (Reynolds et al. 2007). In that study, 8 groups participated and obtained consensus mean $\delta^{30}Si$ values for high-purity Si solids ($\delta^{30}Si_{Diatomite}$: +1.26 ± 0.20 ‰, $\delta^{30}Si_{IRMM\text{-}018}$: -1.65 ± 0.22 ‰, $\delta^{30}Si_{Big\ Batch}$: -10.48 ± 0.54 ‰, uncertainties are 2 s. d.). Those materials are now routinely analyzed and reported when presenting Si isotope data from natural waters, diatom frustules, sponge spicules and minerals. A few rock reference materials are also commonly used as $\delta^{30}Si$ isotopic standards to determine accuracy and reproducibility of solid samples with a complex matrix, especially BHVO-1 and BHVO-2 (e.g. Abraham et al., 2008; Armytage et al., 2012). As exemplified by the offsets between studies measuring $\delta^{30}Si(OH)_4$ in seawater discussed above, these standards are of limited use for identifying sample preparation biases among laboratories analyzing seawater Si isotopes.

In the following we present the first inter-laboratory calibration study for $\delta^{30}Si(OH)_4$ using seawater samples with low (~9 μmol L^{-1}) and high (~113 μmol L^{-1}) $Si(OH)_4$ concentration. The two main goals are to evaluate current reproducibility among laboratories and to establish $\delta^{30}Si(OH)_4$ values for the samples so that they can be analyzed and reported as part of future studies to aid in comparing data generated among and within laboratories over time.

2 METHODS

2.1 Seawater Sampling

The seawater for the intercalibration study was collected at Station ALOHA (22°45´N latitude, 158°00´W longitude) in the North Pacific subtropical gyre. Two large volume seawater samples (60 L each) were collected during the Hawaii Ocean Time series (HOT) cruise 256 (October/November 2013) courtesy of the HOT program using the CTD/rosette sampler aboard the *R/V* Kilo Moana that was equipped with Niskin bottles and a Sea-Bird SBE-9/11 Plus CTD. Samples were collected from 300 m ($ALOHA_{300}$) and 1000 m ($ALOHA_{1000}$) water depth in order to obtain samples with a low and with a high $Si(OH)_4$ concentration based on the known increase in [$Si(OH)_4$] with depth at this location. For each sample seawater from replicate Niskin bottles was pooled in an acid-washed (10% HCl) polyethylene carboy and gravity-filtered into a second acid-washed carboy using AcroPak® filter capsules containing sequential 0.8/0.45μm Supor® membrane filters that had been washed with trace-metal-grade HCl prior to use. Samples were not acidified or preserved as repeated measures of unpreserved samples show no change in either silicic acid concentration or silicon isotopic composition over a period of ten years when kept in the dark (Brzezinski, unpublished).

2.2 Sample Preparation and Silicon Isotope Measurements

At the University of California Santa Barbara (UCSB), the $Si(OH)_4$ concentration of each sample was measured as described by Brzezinski and Nelson (1995). Both $ALOHA_{300}$ and $ALOHA_{1000}$ samples were then aliquoted into 50 mL acid-cleaned polypropylene screw cap tubes, and shipped in groups of 25 tubes each to participating laboratories.

In total, 11 laboratories from 7 countries participated in the study (Table 1). Each group used its own techniques and protocols for sample preparation and Si isotope measurements, as detailed in Table A1. In addition to analyzing the seawater samples, many groups also measured the solid secondary standards Big Batch and Diatomite used in the previous intercalibration of siliceous solids by Reynolds et al. (2007).

All groups used some form of scavenging or precipitation to concentrate Si from the $ALOHA_{300}$ sample and to remove major seawater ions (e.g. Na^+, Cl^-, SO_4^{2-}). All groups

followed similar procedures for $ALOHA_{1000}$ except for group 10 which did not pre-concentrate $ALOHA_{1000}$. Several pre-concentration methods were used: i) a MAGnesium Induced Co-precipitation (MAGIC) method with sodium hydroxide (Karl and Tien, 1992; Georg et al., 2006, de Souza et al., 2012b); ii) a Mg-induced co-precipitation with purified ammonia ($NH_3 \cdot H_2O$, Zhang et al., 2014) and iii) a TEA-Moly precipitation (De La Rocha et al., 1996) during which Si is precipitated as a triethylamine silico-molybdate complex. In the following we will refer to the chemical (NaOH, Ammonia, TEA-Moly) to describe the precipitation method. The most common precipitation method was NaOH, followed by Ammonia and TEA-Moly precipitation.

In order to further purify the samples, most groups using magnesium co-precipitation dissolved the magnesium hydroxide precipitate in a strong acid and then applied column chromatography, using either a cation exchange resin (AG50W-X8; Dowex 50W-X8, AG50W–X12, 200 to 400 mesh) or an anion exchange resin (AG1-X8). Samples precipitated as TEA-Moly were purified by high-temperature combustion to solid SiO_2 in a platinum crucible, followed by the dissolution of the SiO_2 in HF and the precipitation of the dissolved Si as Cs_2SiF_6 (Brzezinski et al., 2006). Depending on the chemical preparation and the mass spectrometer type, the sample volume needed for Si isotope measurements ranged from 8 mL to 2000 mL for $ALOHA_{300}$ and from 1 mL to 200 mL for $ALOHA_{1000}$ with the largest seawater volume being required for measurements by IRMS. For an overview of the different chemical preparation methods, see Table 1. More details about chemical preparation and mass spectrometry methods are given in the appendix (Table A1).

Si isotope measurements were performed on three different mass spectrometer types (Table 1). Four groups used a Neptune or Neptune *Plus* MC-ICP-MS (Thermo Fisher™, Germany), six groups a Nu Plasma MC-ICP-MS (Nu Instruments™, Wrexham, UK; including a Nu Plasma II MC-ICP-MS and a Nu Plasma 1700 HR-MC-ICP-MS) and one group employed a MAT 252 IRMS (Finnigan™, now Thermo Fisher™, Germany). The MC-ICP-MS measurements were performed on solutions containing 10 - 90 μmol L^{-1} Si (0.35–2.5 ppm Si), which resulted in a 2 - 9 V ion beam (on a Faraday cup equipped with a 10^{11} Ω resistor) for elemental Si with m / z of 28, the most abundant stable isotope of Si (atom % ^{28}Si = 92.229 %; Rosman and Taylor, 1998). Most MC-ICP-MS analyses were carried out in 'dry plasma mode' using one of three different desolvating nebulizer systems (CETAC Aridus II™, Nu Instruments DSN-100™, ESI Apex™) to remove the sample solvent before introduction into the plasma.

Only 2 groups employed 'wet plasma mode' (Table A1), which avoids possible blank problems with the desolvating nebulizer system, but is less sensitive (De La Rocha, 2002). On the IRMS, samples are loaded into a modified Kiel III carbonate device as solid Cs_2SiF_6 (6 μmol Si) and decomposed to SiF_4 gas with 98 % sulfuric acid. Electron ionization of SiF_4 in the instrument source creates SiF_3^+ ions measured at 85, 86 and 87 *m / z* (De La Rocha et al. 1996, Brzezinski et al. 2006) with a typical voltage of 4 – 8 V (on a Faraday cup with a 3 x 10^8 Ω resistor) at 85 *m / z* corresponding to $^{28}Si^{19}F_3^+$.

The intensity of the blank was generally below 1% of the sample signal across laboratories (Table A1). All measurements were performed using a standard-sample-bracketing method. For MC-ICP-MS measurements the standard employed was the reference standard NBS28 or an in-house standard that had been calibrated against NBS28. For IRMS measurements samples were run against cryogenically purified commercial SiF_4 gas which had been calibrated against NBS28. NBS28 (NIST Reference Material 8546) is a silica sand that was obtained by the United States Geological Survey from the Corning Glass Company.

Si isotope compositions are reported in the δ-notation using the reference standard NBS28 in parts per thousand,

$$\delta^{30}Si = \left(\left(\frac{R_{sample}}{R_{std}}\right) - 1\right) * 1000 \qquad (1)$$

where R_{sample} is the measured $^{30}Si/^{28}Si$ ratio of the sample and R_{std} is the measured $^{30}Si/^{28}Si$ ratio of the NBS28 standard.

Laboratories pre-concentrated each seawater sample 3 to 10 times. Each pre-concentration was considered to be a replicate when performing statistical tests and when evaluating the external reproducibility for each group (2 s. d., Table 2, A2). The analytical scheme applied to each pre-concentration was as follows: Subsamples of each concentrate were analyzed between 1 and 12 times with the actual number of analyses performed listed as analytical replicates for each pre-concentration in Table A2. Analysis of the subsamples by both IRMS and MC-ICP-MS utilized a standard-sample-bracketing approach, which depending on the laboratory involved 15 to 60 measurements of the subsample bracketed by analyses of the standard. Each set of analytical replicates was averaged providing a mean value for each separate pre-concentration of $ALOHA_{300}$ and of $ALOHA_{1000}$ performed by each laboratory (Table A2).

Analysis of variance (ANOVA) was used to test for difference among means with post hoc tests performed using Tukey's HSD (honest significant difference) method to control type I error rate across multiple comparisons. For each ANOVA Levene's method was used to test for the equality of variance among factors and the Shapiro-Wilk method was used to test that the residuals from each ANOVA model were normally distributed. A significance level of $p = 0.05$ was used throughout. Residuals were normally distributed across all tests and will not be discussed further. However, in some cases the variance across factors was found not to be constant. In those cases, differences among means were re-evaluated using Welch's ANOVA that is not reliant on an assumption of homogenous variances among factors with post hoc testing performed using False Discovery Rate procedures (q-FDR, e.g. Benjamini and Hochberg, 1995; Verhoevenetal., 2005). q-FDR controls the expected proportion of type I errors rather than the probability that such errors will occur which can increase statistical power compared to family-wise error rate techniques for handling multiple comparisons (Benjamini and Hochberg,1995). Statistical analyses were performed using JMP 12 statistical software.

2.3 Mg Doping and Sulfate Addition

Except for one laboratory, all measurements on Neptune mass spectrometers were performed with Mg doping of the sample, whereas only group 10 applied Mg doping to samples measured on a Nu Plasma instrument. Cardinal et al. (2003) showed that Mg isotope mass bias is constant relative to Si isotopes during a MC-ICP-MS analytical session and follows an exponential mass fractionation law. Si isotope ratios ($^{30}Si/^{28}Si$ and $^{29}Si/^{28}Si$) were corrected for mass bias by adding $Mg(NO_3)_2$ to samples and to standards just prior to measurement (Cardinal et al., 2003; Abraham et al., 2008). Mg is added at a concentration that matches the Si content of standards and samples. Between each measurement of Si isotopes ^{24}Mg and ^{25}Mg and/or ^{26}Mg isotopes are measured in dynamic mode with the same integration time as for Si isotopes. The correction to the $^{30}Si/^{28}Si$ ratio $(^{30}Si/^{28}Si)_{corr}$ is calculated as follows:

$$\left(^{30}Si/^{28}Si\right)_{corr} = \left(^{30}Si/^{28}Si\right)_{meas} \times \left(^{30}Si_{AM}/^{28}Si_{AM}\right)^{\varepsilon_{Mg}} \quad (2)$$

where $(^{30}Si/^{28}Si)_{meas}$ is the measured ratio, $^{30}Si_{AM}$ and $^{28}Si_{AM}$ are the atomic masses of ^{30}Si and ^{28}Si. ε_{Mg} is then calculated from the beam intensities on masses 26 and 24 as:

$$\varepsilon_{Mg} = \ln [(^{26}Mg_A/^{24}Mg_A)/(^{26}Mg/^{24}Mg)_{meas}]/[^{26}Mg_{AM}/^{24}Mg_{AM}] \quad (3)$$

where $^{26}Mg_A/^{24}Mg_A$ is the expected ratio of the natural abundances of the isotopes, $(^{26}Mg/^{24}Mg)_{meas}$ is the measured ratio, and $^{26}Mg_{AM}$ and $^{24}Mg_{AM}$ are the atomic masses of ^{26}Mg and ^{24}Mg.

One laboratory (group 2) implemented sulfate doping to overcome the effects of the presence of seawater sulfate ions (Table 1). Van den Boorn et al. (2009) first reported a significant isotopic bias due to the presence of SO_4^{2-} in rock samples after a cation chromatographic purification step. Such a bias was also observed by Hughes et al. (2011) on freshwater samples of dissolved Si, although Georg et al. (2006) and de Souza et al. (2012b) observed no significant matrix effect of SO_4^{2-} on their MC-ICP-MS analyses of Si isotopes from freshwater and seawater samples. In the present study several tests were made to optimize sulfate doping. For group 2, systematic and constant H_2SO_4 additions were performed as for Mg prior to the measurements on the $ALOHA_{1000}$ sample and the NBS28 standard at 1 mmol L^{-1}, which should largely overcome the amount of seawater SO_4^{2-} remaining in the solutions. For the $ALOHA_{300}$ sample where group 2 processed 50 mL of seawater, systematic measurements of SO_4^{2-} were made via ad-hoc doping to reach 1 mmol L^{-1} H_2SO_4. Nitric acid and HCl were also added by group 2 to all samples and standards to reach final concentrations of 0.5 mol L^{-1} each in order to overcome the influence of residual seawater nitrate and chloride ions.

One laboratory (group 1) treated samples with ultraviolet light/ozone to remove dissolved organic carbon (DOC; Table 1) as Hughes et al. (2011) revealed significant biases in $\delta^{30}Si$ data when DOC concentrations significantly exceeded those of dissolved Si.

3 Results

The seawater samples collected from 300 m (300.21 decibar pressure, 13.37°C, salinity 34.311) and 1000 m (1021.65 decibar pressure, 3.88°C, salinity 34.467) at Station ALOHA resulted in the desired range of $Si(OH)_4$ concentrations with measured concentrations of 9.18 ± 0.05 μmol L^{-1} and 112.8 ± 0.5 μmol L^{-1} for $ALOHA_{300}$ and $ALOHA_{1000}$, respectively.

In total, 11 laboratory groups participated in the seawater intercalibration study. The $\delta^{30}Si(OH)_4$ values for $ALOHA_{300}$ and $ALOHA_{1000}$ from each laboratory were in good overall agreement. Average values from individual laboratories for $ALOHA_{300}$ ranged from +1.46 ‰ to

+1.94 ‰, with a mean value of +1.68 ± 0.35 ‰ (2 s. d., results from 9 groups). $\delta^{30}Si(OH)_4$ values for $ALOHA_{1000}$ ranged between +1.10 ‰ and +1.45 ‰ with a mean of +1.24 ± 0.20 ‰ (2 s. d., results from 11 groups; Fig. 1, Table 2). Normal probability plots of the laboratory group means for each sample were highly linear with $R^2 \geq 0.95$ (Fig. 2). Shapiro's tests confirmed that the group averages for $ALOHA_{300}$ were normally distributed (W= 0.966, p = 0.21, where H_0 is that the data are fromm a normal distribution); however, group means for $ALOHA_{1000}$ were not (W = 0.954, p = 0.036). In the latter case the median or modal value may be better measures of central tendency. Median values and interquartile deviations, i.e. 0.5 x (75% quartile – 25% quartile), for $ALOHA_{300}$ and $ALOHA_{1000}$, are +1.66 ± 0.13 ‰ and +1.25 ± 0.06 ‰ respectively (Table 2) with corresponding modal values of 1.66 and 1.22. Values obtained for Big Batch and Diatomite by each group that measured these materials (Table A3) were within the uncertainty bounds of the values established by Reynolds et al. (2007).

The reproducibility of measurements for the seawater samples within individual groups ranged from 0.04 ‰ to 0.24 ‰ for the standard deviations and 0.06 ‰ to 0.13 ‰ for the interquartile deviations with the larger variation generally obtained for $ALOHA_{300}$ (Fig. 1, Table 2). For each sample testing for statistically significant differences in the mean isotope values obtained by each group is confounded as all groups used a single mass spectrometer type negating the use of a two-way ANOVA to simultaneously test for differences among groups and among mass spectrometer types. Testing for differences in the mean isotope values across groups was thus restricted to tests among laboratories using the same mass spectrometer type. Tests for differences among sample preparations methods reveal no significant sample preparation effect (see below) so the effect of preparation was subsumed in the mean square error when examining differences among laboratory groups.

Considering groups that used a Neptune mass spectrometer the ANOVA revealed significant differences among mean values across groups for $ALOHA_{1000}$ ($F = 27.2$, d. f. = 3, $p < 0.001$), but not for $ALOHA_{300}$ ($F = 0.30$, d.f. = 1, $p = 0.59$, note only two groups measured $ALOHA_{300}$ using a Neptune) indicating the presence of small, but statistically significant, biases between laboratories for $ALOHA_{1000}$. However, Levene's test showed unequal variances across groups for both $ALOHA_{300}$ ($F = 8.85$, d.f. = 1, $p = 0.012$) and for $ALOHA_{1000}$ ($F= 3.35$, d.f. = 3, $p = 0.045$) so that the results of the ANOVA should be interpreted with caution. When these data were re-evaluated using Welch's ANOVA the presence of significant differences among

means for $ALOHA_{1000}$ (F= 38.2, d.f. = 3, p <0.0004) and the lack of any significant differences among groups for $ALOHA_{300}$ (F = 0.374, d.f. = 1, p = 0.55) were confirmed. Post hoc tests (Table A4) revealed that differences among laboratories were not consistent between the two seawater samples.

A similar analysis investigating differences among groups using Nu Plasma mass spectrometers showed significant differences among means for both $ALOHA_{300}$ (F = 34.5, d.f. = 5, p < 0.001) and $ALOHA_{1000}$ (F = 6.90, d.f. = 5, p = 0.0004). In both cases the assumption of equality of variances was met (Levine: F= 0.765, d.f. = 5, p = 0.58 and F = 0.421, d.f. = 5, p = 0.83 for $ALOHA_{1000}$ and $ALOHA_{300}$, respectively). Similar to the case for the Neptune, post hoc tests (Table A5) showed that the pattern of significant differences among group means for the Nu Plasma shifted between $ALOHA_{300}$ and $ALOHA_{1000}$. The shifting biases among groups seen for both instruments is also seen in the change in rank order of the mean isotope values obtained by each group between the $ALOHA_{1000}$ and $ALOHA_{300}$ samples (Fig. 1).

An indicator for the quality of $\delta^{30}Si$ measurements is given by the slope of the relationship between $\delta^{30}Si$ and $\delta^{29}Si$ values, as any polyatomic interferences during MC-ICP-MS measurements would lead to an offset from predicted equilibrium or kinetic fractionation line. Least squares linear regression between $\delta^{30}Si(OH)_4$ and $\delta^{29}Si(OH)_4$ produces a slope of 0.5188 ± 0.0184 (s.e., R^2 = 0.98; Fig. 3). Repeating the analysis using reduced major axis model II regression that gives equal weight to errors in both $\delta^{29}Si(OH)_4$ and $\delta^{30}Si(OH)_4$ yields a slope of 0.5131 ± 0.0040 (s.e., R^2 = 0.98).

Figure 4 shows the $\delta^{30}Si(OH)_4$ data for all measurements grouped by mass spectrometer type (Fig. 4a, 4b) and by co-precipitation method (Fig. 4c, 4d). Considering mass spectrometer types the Neptune and Nu Plasma types are replicated across groups while the IRMS is not as IRMS was used by a single group. Thus statistical analysis of mass spectrometer type was only possible for Neptune and Nu Plasma types. Furthermore, as each laboratory used a single mass spectrometer the data from the same group are not independent. To account for this lack of independence an ANOVA with Neptune and Nu Plasma as main effects was performed on the average values obtained by each group weighted by the number of measurements contributing to each mean. Those results show no significant differences between the results obtained on the Neptune versus the Nu Plasma for $ALOHA_{300}$ (F = 0.687, d.f. = 1, p = 0.44) and likewise for $ALOHA_{1000}$ (F = 3.75, d.f. = 1, p = 0.089). In qualitative terms the values obtained by IRMS are

nearly identical to those obtained using the Nu Plasma for $ALOHA_{1000}$, but they appear lower than the averages for either the Nu Plasma or Neptune for $ALOHA_{300}$. That difference is driven by one low value of +1.36 ‰ measured by IRMS (Table A2). If that value is considered an outlier the resulting mean for IRMS becomes closer to that for the other two mass spectrometer types, +1.52 ‰ (Figure 4).

ANOVAs evaluating the effect of different precipitation methods showed no differences among NaOH, Ammonia or TEA-moly procedures for $ALOHA_{1000}$ ($F = 0.27$, d. f. = 2, $p = 0.77$), but a significant difference for $ALOHA_{300}$ ($F = 4.7$, d. f. = 2, $p = 0.014$) driven by a lower mean value for TEA-moly precipitation compared to the other two methods (Table 3, Figure 4). For $ALOHA_{300}$ the significant differences between precipitation methods are driven by one outlier value mentioned above (Table A2). When that value is removed from the analysis no significant differences among precipitation methods ($F = 2.4$, d. f. = 2, $p = 0.10$) are found for $ALOHA_{300}$. We are quick to point out that the ANOVA used to detect differences among precipitation methods necessarily incorporated the effects of groups and of mass spectrometer type into the mean square error as the experimental design is confounded so that these results should be viewed with caution. One group, Group 6, utilized both NaOH and Ammonia co-precipitation methods allowing a direct comparison of methods for this one group. Here too there was no significant difference between precipitation methods ($F = 0.61$, d.f. = 1, $p = 0.49$).

4 Discussion

4.1 General Results

We present the first inter-laboratory study comparing the stable silicon isotope composition of dissolved $Si(OH)_4$ in seawater. Samples with both a relatively low and a relatively high $Si(OH)_4$ concentration were used to evaluate the influence of varying degrees of Si pre-concentration and varying matrix to analyte ratios. The results from the 11 laboratories were in good agreement for both samples, despite the use of different sample preparation and purification methods and different mass spectrometer models (Nu Plasma versus Neptune) and types (MC-ICP-MS versus IRMS). The mean $\delta^{30}Si(OH)_4$ values for $ALOHA_{300}$ and $ALOHA_{1000}$ were +1.68 ± 0.35 ‰ and +1.24 ± 0.20 ‰ (2 s. d.), respectively (Fig. 1, Table 2). Given that the data for $ALOHA_{1000}$ are not normally distributed a better representation of the central tendency is the median. Median values and interquartile deviations for $ALOHA_{300}$ and $ALOHA_{1000}$, are

+1.66 ± 0.13 ‰ and +1.25 ± 0.06 ‰ respectively (Table 2). Modal values are nearly identical (within 0.03 ‰) of corresponding median values (Table 2).

The slope of the least squares fit of $\delta^{30}Si(OH)_4$ versus $\delta^{29}Si(OH)_4$ relationship, 0.5188 is statistically indistinguishable from the theoretical value of 0.5178 for equilibrium control of fractionation ($t = 0.302$, d. f. =19, $p = 0.38$; Thiemens, 1999, Young et al. 2002) and significantly higher than those for kinetic fractionation, i.e. 0.5047 or 0.5092 depending on whether elemental Si or SiO_2 is fractionating, respectively ($t = 4.26$, d. f. = 19, $p = <0.0001$ for Si and $t = 2.90$, d. f. = 19, $p < 0.0001$ for SiO_2, Young et al. 2002). The slope of the reduced major axis regression, 0.5131, is statistically indistinguishable from both the theoretical value for equilibrium fraction ($t = 1.17$, d. f. = 19, $p = 0.13$) and the kinetic fractionation of SiO_2 ($t = 0.94$, d. f. = 19, $p = 0.97$), but it was statistically larger than the theoretical value for the kinetic fractionation of elemental Si ($t = 2.10$, d. f. = 19, $p < 0.00001$). For reference the Bonferroni corrected p value for these six comparisons is 0.008. Thus, the data lack the precision necessary to discriminate between control by equilibrium or kinetic fractionation. Ultimately, the fractionation of $Si(OH)_4$ in the sea should be kinetically controlled given the strong role of biology in the process (Nelson et al.1995).

The tight relationship between $\delta^{30}Si(OH)_4$ and $\delta^{29}Si(OH)_4$ relationship does indicate insignificant isobaric interference problems during Si isotope analysis. External reproducibility (2 s. d.) during this study (0.20 ‰ and 0.35 ‰ for $ALOHA_{1000}$ and $ALOHA_{300}$, respectively) were similar to those obtained during the inter-laboratory comparison of Si isotopes in pure siliceous solid materials by Reynolds et al. (2007), where 2 s. d. uncertainty values of 0.22 ‰, 0.16 ‰ and 0.54 ‰ were obtained for the standards IRMM-018, Diatomite and Big Batch, respectively. Analyzing both $ALOHA_{300}$ and $ALOHA_{1000}$ as a routine part of future studies of seawater Si isotopes will allow potential biases to be quantified, facilitating comparisons among data sets.

The suite of methodologies used to analyze the isotopic composition of Si in the seawater samples all yielded robust results. Comparison of the data obtained from the low and high concentration samples suggests that further improvement may be possible. Overall $ALOHA_{1000}$ shows a better reproducibility (± 0.20 ‰ s.d., 0.05 ‰ i.q.d) than $ALOHA_{300}$ (± 0.35 ‰ s.d., 0.13 ‰ i.q.d.) among laboratories and within each laboratory (Fig. 1, Table 2). Small, but statistically significant, differences in the mean isotope values among laboratories were

detected for both samples (Table A4). Moreover, the number and magnitude of significant differences changed between the low and high concentration samples (Table A4). Together these results imply that differences in how the two samples were processed marginally influenced the results.

The main difference in sample preparation between $ALOHA_{300}$ and $ALOHA_{1000}$ was the larger sample volume processed for $ALOHA_{300}$ (Table A1). The volume of seawater used for pre-concentration scales inversely with the $Si(OH)_4$ concentration in the sample such that larger volumes are processed for samples with low Si concentration. To the extent that they are not removed during the chromatographic purification of Si, the carryover of seawater ions (e.g. Mg^{2+}, Na^{+}, Ba^{2+}, Cl^{-}, SO_4^{2-}) will be a function of the sample volume processed, altering the ratio of these ions to the analyte Si in the final sample which may produce matrix effects during measurements (see Methods). As most groups use a cation exchange resin as the final purification step (Table 1), residual anions are likely present.

Another possible cause of the larger variance of the measurements of $ALOHA_{300}$ could be the higher DOC to Si ratio in the shallow sample. Any element remaining in the solution analyzed can compete with analyte for ionization within the plasma and thus can potentially induce a matrix effect on isotopic mass bias. Hughes et al. (2011) showed that a DOC:Si mass ratio (as C:Si) above 0.6 can interfere with $\delta^{30}Si$ measurements. DOC concentrations measured on the same cruise and at the same depths as sampled for Si isotopes were 48 and 37 μmol C L^{-1} for $ALOHA_{300}$ and $ALOHA_{1000}$, respectively (C. A. Carlson, pers. com.), which are three orders of magnitude lower than in the samples analyzed by Hughes et al. (2011). However, DOC/Si mass ratios (C/Si) were 2.2 and 0.1 for $ALOHA_{300}$ and $ALOHA_{1000}$, respectively. Those ratios imply a potential for interference from DOC in $ALOHA_{300}$ if DOC is concentrated at the same efficiency as Si during the sample pre-concentration procedure. Detailed investigations into these and other possible interferences may improve the analytical precision obtained for low concentration samples.

4.2 Potential Instrument Biases

Measurements on the Neptune (mean = +1.18 ± 0.18 ‰) and the Nu Plasma (mean = +1.28 ± 0.18 ‰) show a slight and only marginally significant ($p = 0.089$) offset for $ALOHA_{1000}$ with the values from the Neptune being lower by 0.1 ‰. For $ALOHA_{300}$ the mean value on the Neptune

is also lower than on the Nu Plasma by 0.1‰ (Table 3), but in this case the difference is far from statistically significant given the larger variance of the measurements for the shallow sample. One possible explanation for this offset could be the applied Mg doping of the sample, which is mainly conducted for measurements on the Neptune (except for group 11), to correct for the instrumental mass bias (Cardinal et al. 2003). This possibility was investigated by examining the results for Group 11, which performed Si isotope analysis on a Neptune without Mg doping. The mean value for this group was slightly higher +1.27 ± 0.05 ‰ (2s.d.), than the Neptune mean. Only one group (Group 10) applied Mg doping using a Nu Plasma, which resulted in a mean value of +1.45 ± 0.17 ‰, higher than the average δ^{30}Si value of +1.28 ± 0.18 ‰ obtained by groups using the Nu Plasma without Mg doping. The results are thus inconclusive, and it is not clear whether Mg doping or an instrument bias caused the small offset between the results from the Neptune and Nu Plasma instruments.

The average $\delta^{30}Si(OH)_4$ value from IRMS match the average from the Nu Plasma for $ALOHA_{1000}$, but they are lower than both the Nu Plasma or Neptune data for $ALOHA_{300}$. It is difficult to draw firm conclusions from these similarities and differences given the very large difference in the volume of seawater processed for measurement by IRMS compared to the other instrument types (Table 3).

4.3 Possible Improvement of Chemical Preparation and δ^{30}Si Measurements

There are several approaches to reduce "matrix effects" in MC-ICP-MS measurements caused by remnants of DOC and seawater ions in samples (Cardinal et al., 2007, Hughes et al., 2011). Methods that further reduce the ion concentrations (cations and anions) may thus be beneficial or ion concentrations in the sample solution could be measured and the samples doped prior to measurement, though the latter may be cumbersome for studies with large numbers of samples. Alternatively, a sequential cation-anion-exchange chromatography purification procedure, such as has been tested by some groups for $\delta^{30}Si(OH)_4$ (N. Estrade, pers. comm.), may be a promising approach. Closset (2015) showed that the contribution of Cl^- originating from seawater can be neglected when HCl is used to dissolve the brucite produced during Mg co-precipitation as the Cl^- from the acid is present in large excess (up to 0.5 mol L^{-1}) compared to remaining Cl^- from seawater. Similarly, the occurrence of NO_3^- in seawater is negligible when HNO_3 (0.5 mol L^{-1}) is used as a solvent in both the samples and standards. In the present study

group 2 employed a mixture that was 0.5 mol L^{-1} HCl, 0.5 mol L^{-1} HNO_3 and 1 mmol L^{-1} H_2SO_4 to simultaneously compensate for the presence of Cl^-, NO_3^- and SO_4^{2-}.

The concentration of SO_4^{2-} ions remaining after chemical purification of the Si (i.e. not collected by cation exchange resin) depends on the volume of seawater used for the NaOH and Ammonia methods. There is, however, no simple relationship between total sample volume processed and final SO_4^{2-} concentration, since most seawater is discarded during the pre-concentration procedure. Some laboratories also observed that the presence of high SO_4^{2-} (higher than 0.5 mmol L^{-1}) may cause a negative shift in the baseline of ^{29}Si and ^{30}Si due to the high ^{32}S signal. More importantly, this impact will directly alter the Si^+ signal intensity and is different from the matrix effect, and cannot be corrected using the matrix-match approach (Zhang A., data unpublished). The influence of residual ions also varies with the number of co-precipitations employed as the two-step NaOH process developed by Reynolds et al. (2006) significantly reduces the final seawater volume from which Si is stripped compared to a one step co-precipitation. Furthermore, a general treatment of seawater sample with ultra violet light, ozone or peroxide to reduce the influence of dissolved organic matter, as already suggested by Hughes et al. (2011) may be beneficial.

The IRMS method is largely free of "matrix effects". Interference from $SiOF_2$ is rare as a significant signal at *m / z* 83 that would indicate the presences of the compound (see above) are rarely observed. The major challenge with the Cs_2SiF_6 IRMS method is the large sample size required compared to MC-ICP-MS. When less than 5 μmoles of Cs_2SiF_6 are analyzed the resulting $\delta^{30}Si$ values are significantly biased to higher values (Brzezinski et al., 2006). This is not a limitation of the instrument, as the Kiel III/ MAT 252 combination is capable of analyzing at least an order of magnitude lower amount of Si. The reason for the apparent fractionation of small samples is unknown. Overcoming this limitation would allow seawater sample volumes similar to those currently employed for MC-ICP-MS analysis. The lower limit of sample size would then essentially only be determined by the mass of Si necessary to quantitatively precipitate Cs_2SiF_6.

4.4 Best Practices during MC-ICP-MS Measurements

The major challenges during MC-ICP-MS measurements leading to lower accuracy and precision are i) molecular interference at *m / z* ^{28}Si ($^{14}N_2$, $^{12}C^{16}O$), ^{29}Si ($^{14}N_2{}^1H$, $^{12}C^1H^{16}O^{15}N^{14}N$)

and ^{30}Si ($^{14}N^{16}O$) and ii) variable mass-dependent fractionation in the instrument (mass-bias, see also Cardinal et al. 2003). To handle possible problems with interfering compounds the matrix blank should not exceed 1% of the sample sensitivity and it should be routinely measured and subtracted from the measurement signal. Furthermore the achieved resolving power (10% peak valley definition) of the mass spectrometer should be above 3500 in order to clearly separate molecular interference masses. All of these issues are also influenced by operating condition ("plasma conditions"), non-analyte composition of the particular sample ("matrix effect") and the amount of material that is introduced into the instrument ("mass-load effect"), which is determined by the Si concentration introduced into the instrument by the sample gas flow. A study by Zhang et al. (2015b) also demonstrated that the sample gas flow has an effect on the production of polyatomic ions besides its obvious effects on sensitivity and stability. The importance of the energetic/thermal "plasma conditions" during ICP-MS measurements for precise and accurate stable isotope measurements was recently shown by Fietzke et al. (2015). Therefore, in addition to the elemental purity of the sample and the Si concentration introduced into the instrument, plasma conditions should be monitored carefully in order to improve the accuracy and precision of $\delta^{30}Si$ measurements. This may require allowing the instrument to stabilize for several hours before measurements.

4.5 Recommendations

The intercalibration results show a very good precision within all participating groups taking into account the external reproducibility of the individual measurements. However, small but statistically significant differences among mean values across groups were observed for both samples. Such differences can be rigorously quantified through routine analysis of these reference waters as part of future studies of $\delta^{30}Si(OH)_4$ distributions in the ocean. This is particularly important for international programs such as GEOTRACES for which global data from multiple laboratories are often combined for analysis. It is recommended that future studies analyzing $\delta^{30}Si(OH)_4$ in seawater also analyze $ALOHA_{300}$ and $ALOHA_{1000}$ and report these results to facilitate and evaluate comparability of data between laboratories. While the use of ALOHA samples is needed to validate the seawater processing procedures, analytical conditions and instrument stability should first be checked for each analytical session by measuring secondary reference materials such as Diatomite and Big Batch (Reynolds et al., 2007) which are

more readily available. ALOHA samples, Diatomite and Big Batch can be obtained from Mark Brzezinski at UCSB. Finally, a plan for reference water renewal must be developed to facilitate intercalibration efforts in the future.

Acknowledgements

Our thanks to Matthew Church for his help in obtaining seawater samples from Hawaii Ocean Time Series station ALOHA. This work was supported by OCE-1233029 from the US National Science Foundation, Chemical Oceanography Program to MB. DC thanks for their financial support the EU FP7 (CIG #294146) and IPSL. GFDS is funded by a Marie Skłodowska-Curie Research Fellowship under EU Horizon2020 (SOSiC, GA #708407). PG and MF acknowledge funding by the Collaborative Research Centre 754 “Climate- Biogeochemistry interactions in the Tropical Ocean” (www.sfb754.de), supported by the Deutsche Forschungsgemeinschaft (DFG). The work by JNS was supported by the "Laboratoire d'Excellence" LabexMER (ANR-10-LABX-19) and co-funded by a grant from the French government under the program "Investissements d'Avenir", and by a grant from the Regional Council of Brittany (SAD programme). AZ and JZ were supported by the Ministry of Science and Technology of China (grant 2011CB409801). QL and DL acknowledge financial support from the National Natural Science Foundation of China (No. 21422509 and 91543104). RF and DW acknowledge financial support from the Natural Sciences and Engineering Research Council of Canada and NE benefitted from a post-doctoral fellowship from NSERC (CREATE - MAGNET). CE and KP acknowledge the funding from ICBM (Univ. of Oldenburg) and the Max Planck Institute for Marine Microbiology Bremen.). PA, EK and MS acknowledge the financial support of Vetenskapsrådet, Sweden, for funding the Vegacenter at NRM Stockholm (grant #829-2011-6326). We also would like to acknowledge William Rice and Wilfried Rickels for the improvement of the statistics.

References

Abraham, K., Opfergelt, S., Fripiat, F., Cavagna, A.-J., De Jong, J. T. M., Foley, S. F., et al. (2008). δ^{30}Si and δ^{29}Si Determinations on USGS BHVO-1 and BHVO-2 Reference Materials with a New Configuration on a Nu Plasma Multi-Collector ICP-MS. *Geostandards and Geoanalytical Research*, *32*(2), 193–202.

Albarède, F., Telouk, P., Blichert-Toft, J., Boyet, M., Agranier, A., & Nelson, B. (2004). Precise and accurate isotopic measurements using multiple-collector ICPMS. *Geochimica et Cosmochimica Acta*, *68*, 2725–2744.

Armytage, R. M. G., Georg, R. B., Williams, H. M., & Halliday, A. N. (2012). Silicon isotopes in lunar rocks: Implications for the Moon's formation and the early history of the Earth. *Geochimica et Cosmochimica Acta*, *77*, 504–514. http://doi.org/10.1016/j.gca.2011.10.032

Benjamini, Y., Hochberg, Y., 1995. Controlling the false discovery rate: a practical and powerful approach to multiple testing. Journal of the Royal Statisical Society 57 (1), 289–300. Boyd, P., LaRoche, J., Gall, M., Frew

Beucher, C. P., Brzezinski, M. A., & Jones, J. L. (2008). Sources and biological fractionation of Silicon isotopes in the eastern Equatorial Pacific. *Geochimica et Cosmochimica Acta*, *72*, 3063–3073.

Brzezinski, M. A., Jones, J. L. J., Beucher, C. P. C., Demarest, M. S. M., & Berg, H. L. H. (2006). Automated determination of silicon isotope natural abundance by the acid decomposition of cesium hexafluosilicate. *Analytical Chemistry, 78*(17), 6109–6114.

Brzezinski, M. A., & Jones, J. L. (2015). Coupling of the distribution of silicon isotopes to the meridional overturning circulation of the north Atlantic ocean. *Deep Sea Research Part II: Topical Studies in Oceanography*. 116, 79-88.

Brzezinski, M.A., Nelson, D.M., 1995. The annual silica cycle in the Sargasso Sea near Bermuda. *Deep-Sea Reearch. I* 42, 1215–1237.

Cao, Z., Frank, M., & Dai, M. (2015). Dissolved silicon isotopic compositions in the East China Sea: Water mass mixing vs. biological fractionation. *Limnology and Oceanography*, *60*(5), 1619–1633.

Cardinal, D., Alleman, L. Y., De Jong, J., Ziegler, K., & André, L. (2003). Isotopic composition of silicon measured by multicollector plasma source mass spectrometry in dry plasma mode. *Journal of Analytical Atomic Spectrometry*, *18*, 213–218.

Cardinal D., Alleman, L.Y., Dehairs F., Svoye, N., Trull, T.W., Andre, L. (2005) Relevance of silicon isotopes to Si-nutrient utilization and Si-source assessment in Antarctic waters. *Global Biogeochemical Cycles*, 19, GB2007, doi:10.1029/2004GB002364

Closset I. (2015). The biogeochemical silicon cycle in the Southern Ocean tracked by isotopic approaches. Ph. D. thesis. Université Pierre & Marie Curie, 222p.

De La Rocha, C., Brzezinski, M. A., & DeNiro, M. J. (1996). Purification, Recovery, and Laser-Driven Fluorination of Silicon from Dissolved and Particulate Silica for the Measurement of Natural Stable Isotope Abundances. *Analytical Chemistry*, 68, 3746–3750.

De La Rocha, C., Brzezinski, M. A., & DeNiro, M. J. (2000). A first look at the distribution of stable isotopes of silicon in natural waters. *Geochimica et Cosmochimica Acta*, *64*, 2467–2477.

De La Rocha, C. (2002). Measurement of silicon stable isotope natural abundances via multicollector inductively coupled plasma mass spectrometry (MC-ICP-MS). *Geochemistry Geophysics Geosystems*, *3*(8), GC000310. http://doi.org/10.1029/ 2002 GC000310.

De La Rocha, C. L., Brzezinski, M.A., DeNiro, M.J. (2006). Opal-based isotopic proxies of paleoenvironmental conditions. *Global Biogeochemical Cycles*, 20, GB4S09, doi:10.1029/2005GB002664

De La Rocha, De, C. L., Bescont, P., Croguennoc, A., & Ponzevera, E. (2011). The silicon isotopic composition of surface waters in the Atlantic and Indian sectors of the Southern Ocean. *Geochimica et Cosmochimica Acta*, *75*(18), 5283–5295.

de Souza, G. F., Reynolds, B. C., Johnson, G. C., Bullister, J. L., & Bourdon, B. (2012a). Silicon stable isotope composition traces Southern Ocean export of Si to the eastern South Pacific thermocline. *Biogeosciences*, 9, 4199-4213.

de Souza, G. F., Reynolds, B. C., Rickli, J., Frank, M., Saito, M. A, Gerringa, L. J. A., & Bourdon, B. (2012b). Southern Ocean control of silicon stable isotope distribution in the deep Atlantic Ocean. *Global Biogeochemical Cycles*, 26, doi: 10.1029/2011GB004141

de Souza, G. F., Slater, R. D., Dunne, J. P., & Sarmiento, J. L. (2014). Deconvolving the controls on the deep ocean's silicon stable isotope distribution. *Earth and Planetary Science Letters*, *398*, 66–76.

de Souza, G. F., Slater, R. D., Hain, M. P., Brzezinski, M. A., & Sarmiento, J. L. (2015). Earth and Planetary Science Letters. *Earth and Planetary Science Letters*, *432*, 342–353.

Ehlert, C., Grasse, P., Guitiérrez, D., Salvatteci, R., & Frank, M. (2015). Nutrient utilisation and weathering inputs in the Peruvian upwelling region since the Little Ice Age. *Climate of the Past*, *11*, 1–16.

Engstrom E., Rodushkin I., Baxter D.C., Ohlander, B. (2006) Chromatographic purification for the determination of dissolved silicon isotopic compositions in natural waters by high resolution multicollector inductively coupled plasma mass spectrometry. *Analytical Chemistry*, 75, 250-257.

Fietzke, J., & Frische, M. (2015). Experimental evaluation of elemental behavior during LA-ICP-MS: influences of plasma conditions and limits of plasma robustness. *Journal of Analytical Atomic Spectrometry*, *31*, 234–244.

Gao, S., Wolf Gladrow, D. A., & Völker, C. (2016). Simulating the modern δ^{30}Si distribution in the oceans and in marine sediments. *Global Biogeochemical Cycles*, (GB005189). http://doi.org/10.1002/2015GB005189

Georg, R., Reynolds, B., Frank, M., & Halliday, A. (2006). New sample preparation techniques for the determination of Si isotopic compositions using MC-ICPMS. *Chemical Geology*, 235(1-2), 95–104.

Grasse, P., Ehlert, C., & Frank, M. (2013). The influence of water mass mixing on the dissolved Si isotope composition in the Eastern Equatorial Pacific. *Earth and Planetary Science Letters*, *380*, 60–71.

Holzer, M., & Brzezinski, M. A. (2015). Controls on the silicon isotope distribution in the ocean: New diagnostics from a data-constrained model. *Global Biogeochemical Cycles*, *29*(3), 267–287.

Hughes, H. J., Delvigne, C., Korntheuer, M., de Jong, J., André, L., & Cardinal, D. (2011). Controlling the mass bias introduced by anionic and organic matrices in silicon isotopic measurements by MC-ICP-MS. *Journal of Analytical Atomic Spectrometry*, *26*(9), 1892–1896.

Hulston J. R. and Thode H. G. (1965). Variations in the S^{33}, S^{34}, and S^{36} contents of meteorites and their relation to chemical and nuclear effects. *J. Geophys. Res.* **70,** 3475–3484.

Karl, & Tien, G. (1992). MAGIC: A sensitive and precise method for measuring dissolves phosphorus in aquatic environments. *Limnology and Oceanography*, 37, 105–116.

Maier, E., Chapligin, B., Abelmann, A., Gersonde, R., Esper, O., Ren, J., et al. (2013). Combined oxygen and silicon isotope analysis of diatom silica from a deglacial subarctic Pacific record. *Journal of Quaternary Science*, *28*(6), 571–581.

Nelson, D. M., Tréguer, P., Brzezinski, M. A., Leynaert, A. & Quéguiner, B. 1995. Production and dissolution of biogenic silica in the ocean: Revised global estimates, comparison with regional data and relationship to biogenic sedimentation. *Global Biogeochem. Cycles* 9(3):359-72.

Reynolds, B., Frank, M., & Halliday, A. (2006). Silicon isotope fractionation during nutrient utilization in the North Pacific. *Earth and Planetary Science Letters*, *244*(1-2), 431–443.

Reynolds, B. C., Aggarwal, J., Andr, L., Baxter, D., Beucher, C., Brzezinski, M. A., et al. (2007). An inter-laboratory comparison of Si isotope reference materials. *Journal of Analytical Atomic Spectrometry*, *22*(5), 561.

Reynolds, B. C., Frank, M., & Halliday, A. N. (2008). Evidence for a major change in silicon cycling in the subarctic North Pacific at 2.73 Ma. *Paleoceanography*, *23*(4), PA4219. http://doi.org/10.1029/2007PA001563

Rosman, K. J. R.; Taylor, P. D. P. (1998). Isotopic composition of the elements 1997. *Pure Applied Chemistry*, *70*, 217-236.

Singh, S. P., Singh, S. K., Bhushan, R., & Rai, V. K. (2015). Dissolved silicon and its isotopes in the water column of the Bay of Bengal: Internal cycling versus lateral transport. *Geochimica et Cosmochimica Acta*, 151, 172-191.

Sun, X., Olofsson, M., Andersson, P. S., Fry, B., Legrand, C., Humborg, C., Mörth, C.-M. 2014. Effects of growth and dissolution on the fractionation of silicon isotopes by estuarine diatoms. *Geochimica et Cosmochimica Acta*, 130,156–166.

Thiemens, M. H. (1999). Mass-Independent Isotope Effects in Planetary Atmospheres and the Early Solar System. *Science*, *283* (5400), 341–345.

Tréguer, P. J., & La Rocha, De, C. L. (2013). The World Ocean Silica Cycle. *Annual Review of Marine Science*, *5*(1), 477–501.

van den Boorn, S. H. J. M., Vroon, P. Z., & van Bergen, M. J. (2009). Sulfur-induced offsets in MC-ICP-MS silicon-isotope measurements. *Journal of Analytical Atomic Spectrometry* 24, doi: 10.1039/b816804k.

Verhoeven, K.J.F., Simonsen, K.L., McIntyre, L.M., 2005. Implementing false discovery rate control: increasing your power. Oikos 108, 643–647.

Young, E. D., Galy, A., & Nagahara, H. (2002). Kinetic and equilibrium mass-dependent isotope fractionation laws in nature and their geochemical and cosmochemical significance. *Geochimica Et Cosmochimica Acta*, *66*(6), 1095–1104.

Zhang, A., Zhang, J., Zhang, R., & Xue, Y. (2014). Modified enrichment and purification protocol for dissolved silicon isotope determination in natural waters. *Journal of Analytical Atomic Spectrometry*. doi:10.1039/C4JA00122B

Zhang, A., Zhang, J., Hu, J., Zhang, R., & Zhang, G. (2015a) Silicon isotopic chemistry in the Changjiang Estuary and coastal regions: Impacts of physical and biogeochemical processes on the transport of riverine dissolved silica. *Journal of Geophysical Research: Oceans*, 10.1002/2015JC011050

Zhang, A., Zhang, J., Zhang, R., & Xue, Y. (2015b). Determination of stable silicon isotopes using multi-collector inductively coupled plasma mass spectrometry. *Chinese Journal of Analytical Chemistry*, 43(9): 1353-1359.

Figure Captions:

Figure 1. $\delta^{30}Si(OH)_4$ results from all groups for $ALOHA_{300}$ (open circles) and $ALOHA_{1000}$ (filled circles). The long black vertical solid line indicates the mean value of all measurements for $ALOHA_{1000}$ and the long dashed line that for $ALOHA_{300}$. The data points represent the individual $\delta^{30}Si(OH)_4$ values from Table A2. Short vertical solid lines are the means obtained by individual laboratories for the two samples. Uncertainty in the mean for all measurements for each sample (2 s. d.) is indicated by the horizontal bars at the top of the figure.

Figure 2. Z scores as a function of $\delta^{30}Si(OH)_4$ for $ALOHA_{300}$ (open circles) and $ALOHA_{1000}$ (filled circles).

Figure 3. Plot of $\delta^{30}Si(OH)_4$ versus $\delta^{29}Si(OH)_4$ for $ALOHA_{300}$ (open circle) and $ALOHA_{1000}$ (filled circle; error bars are 2 s. d.). Solid line is the result of least-squares linear regression with a slope of 0.5188 ± 0.0184 (s.e., $R^2 = 0.98$). The lower and upper 95 % confidence intervals are given as dashed black lines. The kinetic fractionation line has a slope of 0.5092 (intercept of zero) for Si (dashed red line) and the equilibrium fractionation line has a slope of 0.5178 (intercept of zero) for Si (solid red line). Regression line obtained by analysis using reduced major axis model II regression yields a slope of 0.5131 ± 0.0040 (s.e., $R^2 = 0.98$; not displayed in the figure).

Figure 4. Boxplots showing $\delta^{30}Si(OH)_4$ data sorted by different mass spectrometer types for a) $ALOHA_{300}$ and for b) $ALOHA_{1000}$. Data sorted by different precipitation methods for c) $ALOHA_{300}$ and d) $ALOHA_{1000}$. On the boxplots the median values (black) and the mean values (grey) are displayed. For $ALOHA_{300}$ a) and c) show data for IRMS and TEA-Moly with (grey boxplot) and without outlier (black boxplot). Here, the mean value (which equals the median) is indicated by a superscript star. The value next to each boxplot indicates the median (black) and the mean (grey), respectively. The number of included data points (n) is given below each boxplot. Raw data are presented in Table 3

Table 1: Summary of the different participating laboratory groups and methods for sample preparation and mass spectrometry.

No.	Lab	Country	Resposible person	Sample Introduction	Mass spectrometry	Precipitation Method	Further preparation	Extras	References
1	MPI Oldenburg	Germany	Claudia Ehlert, Katharina Pahnke	Wet-plasma	Neptune *Plus*	NaOH	Cation Exchange Resin (AG50W-X8)	H_2O_2/UV treatment/Mg doping	Georg et al. 2006; Hughes et al. 2011
2	LOCEAN/LSCE	France	Damien Cardinal, Ivia Closset,	Apex, Dry-plasma	Neptune *Plus*	NaOH	Cation Exchange Resin (AG50W-X8)	Mg//SO_4^{2-} Doping	Karl and Tien 1992; Georg et al. 2006; Hughes et al. 2011
3	Unité de Recherche Géosciences Marines, IFREMER and Université de Brest	France	Jill Sutton	Apex, Dry- plasma	Neptune	TEA-Moly	Anion Exchange Resin (AG1-X8)	Mg doping	Cardinal et al. 2005; Engström et al. 2006; De La Rocha et al. 2006; De LaRocha et al. 2011
4	ETH Zürich	Switzerland	Florian Wetzel, Gregory de Souza	DSN-100, Dry-plasma	Nu Plasma 1700	NaOH	Cation Exchange Resin (AG50W-X8)		Georg et al. 2006; deSouza et al. 2012
5	Swedish Museum of Natural History	Sweden	Per Andersson, Xiaole Sun	Wet-plasma	Nu Plasma II	NaOH	Cation Exchange Resin (AG50W-X8)		Georg et al. 2006; Sun et al. 2014
6	GEOMAR Helmholz Institute for Ocean Research	Germany	Patricia Grasse, Martin Frank	Aridus II, Dry-plasma	Nu Plasma II	NaOH/NH_4	Cation Exchange Resin (AG50W-X8)		Karl and Tien 1992; Georg et al. 2006; Zhang et al. 2014
7	University of British Columbia	Canada	Nicolas Estrade	Aridus II, Dry-plasma	Nu Plasma 1700	NH_4	Cation Exchange Resin (AG50W-X8)		Karl and Tien 1992; Zhang et al. 2014
8	University of California Santa Barbara	US	Janice Jones, Patricia Grasse, Mark Brzezinski	Dual-inlet gas-source	Kiel III MAT 252	TEA-Moly	HF dissolution, then $CsSiF_6$ precipitation		De LaRocha et al. 1996; Brzezinski et al. 2006
9	Xiamen University	China	Minhan Dai, Zhouling Zang	Dry-plasma	Nu Plasma II	NaOH	Cation Exchange Resin (AG50W-X8)		Karl and Tien 1992; Georg et al. 2006
10	Research Center for Eco-Environmental Sciences,CAS Beijing	China	Qian Liu	DSN-100, Dry-plasma	Nu Plasma II	NaOH	Cation Exchange Resin (Dowex50W-X8)		Karl and Tien 1992; Georg et al. 2006
11	State Key Laboratory of Estuarine and Coastal Research, Shanghai	China	Anyu Zhang	Dry-plasma	Neptune	NH_4	Cation Exchange Resin (Dowex50W-X8)		Georg et al. 2006; Zhang et al. 2014; Zhang et al. 2015

Table 2: Summary of mean Si isotope values ($\delta^{30}Si$, $\delta^{29}Si$), the associated 2σ analytical uncertainty (2 s.d.), number of chemical preparations (N) and the number of measurements (n) obtained by each laboratory group for $ALOHA_{300}$ and $ALOHA_{1000}$. Overall mean, uncertainty about the mean (2 s.d.), median as well as the interquartile deviation (IQD) for all groups are given at the bottom of the table. NaN indicates data not available (for a compilation of all measurements see Table A2).

	Aloha$_{300}$							**Aloha$_{1000}$**						
Group No.	**$\delta^{30}Si$**	**2 s.d.**	**$\delta^{29}Si$**	**2 s.d.**	**$\delta^{29}Si/\delta^{30}Si$**	**N**	**n**	**$\delta^{30}Si$**	**2 s.d.**	**$\delta^{29}Si$**	**2 s.d.**	**$\delta^{29}Si/\delta^{30}Si$**	**N**	**n**
1	NaN	NaN	NaN	NaN	NaN	NaN	NaN	1.10	0.07	0.63	0.07	0.57	4	4
2	1.66	0.10	0.84	0.05	0.50	6	12	1.10	0.07	0.56	0.02	0.51	5	15
3	NaN	NaN	NaN	NaN	NaN	NaN	NaN	1.16	0.16	0.59	0.09	0.51	3	9
4	1.64	0.13	0.87	0.05	0.53	4	12	1.17	0.20	0.62	0.10	0.53	3	12
5	1.51	0.12	0.80	0.08	0.53	3	11	1.23	0.08	0.64	0.04	0.52	4	15
6	1.78	0.18	0.89	0.18	0.50	6	6	1.26	0.12	0.68	0.09	0.54	5	5
7	1.92	0.08	1.02	0.12	0.53	5	14	1.25	0.07	0.65	0.07	0.52	6	31
8	1.46	0.17	0.75	0.09	0.51	3	10	1.29	0.04	0.66	0.02	0.51	4	25
9	1.94	0.12	0.99	0.08	0.51	8	16	1.31	0.15	0.68	0.09	0.52	10	20
10	1.53	0.17	0.79	0.11	0.52	3	9	1.45	0.17	0.76	0.16	0.53	3	9
11	1.69	0.24	0.85	0.17	0.50	8	8	1.27	0.05	0.65	0.03	0.51	8	72
Mean	**1.68**		**0.87**		**0.52**			**1.24**		**0.65**		**0.52**		
2 s.d.	**0.35**		**0.10**					**0.20**		**0.10**				
Median	**1.66**		**0.85**					**1.25**		**0.65**				
Modal Value	**1.66**		**0.85**					**1.22**		**0.65**				
IQD	**0.13**		**0.05**					**0.05**		**0.02**				

Table 3: Statistics for $\delta^{30}Si(OH)_4$ values sorted by different instrument types and precipitation methods (for details see Appendix 2). NaN denotes sample not available.

Grouped by Instrument						
		$Aloha_{300}$			**$Aloha_{1000}$**	
	Neptune	**Nu**	**IRMS**	**Neptune**	**Nu**	**IRMS**
Median	1.64	1.81	1.51	1.15	1.28	1.28
Mean	1.68	1.78	1.46	1.18	1.28	1.29
2 s.d.	0.19	0.36	0.17	0.18	0.18	0.04
Min	1.52	1.45	1.36	1.07	1.08	1.27
Max	1.86	2.05	1.52	1.30	1.55	1.31
N	14	29	3	20	31	4

Grouped by Precipitation						
		$Aloha_{300}$			**$Aloha_{1000}$**	
	MAGIC	**Ammonia**	**TEA-Moly**	**MAGIC**	**Ammonia**	**TEA-Moly**
Median	1.69	1.82	1.51	1.25	1.27	1.27
Mean	1.73	1.78	1.46	1.24	1.26	1.23
2 s.d.	0.34	0.30	0.17	1.25	0.06	0.16
Min	1.45	1.52	1.36	1.07	1.20	1.10
Max	2.05	1.97	1.52	1.55	1.30	1.31
N	30	13	3	32	16	7

Table A1: Detailed Overview of chemical preparation and measurement methods (1/5; Nu Plasma)

Group	**4**	**5**	**6**	**7**	**9**	**10**
Sample Vol. ($Aloha_{300}$)	50 ml	50ml	30ml	12ml	15ml	15ml
Sample Vol. ($Aloha_{1000}$)	10 ml	10ml	10ml	12ml	10ml	10ml
Precipitation Method	MAGIC	MAGIC	MAGIC	MAGIC	MAGIC	MAGIC
	Sodium hydroxide	Ammonium Hydroxid	Ammonium & Sodium Hydroxid	Ammonium Hydroxid	Sodium Hydroxid	Ammonium Hydroxid
Column Chemistry	Cation Exchange Resin	Cation Exchange Resin	Cation Exchange Resin	Cation Exchange Resin	Cation Exchange Resin	Cation Exchange Resin
	AG50W-X8, 200-400 mesh	AG50W-X12	AG50W-X8, 200-400 mesh	AG50W-X8, 200-400 mesh	AG50W-X8, 200-400 mesh	Dowex50W-X8
Amount Si (µg) introduced into machine	2.5 µg	0.6 to 1.6 µg	2.5 µg	1.4 µg		1.8 µg
Mg Doping (yes/no)	no	no	no	no	no	yes
Extras		$Aloha_{300}$ evaporated after column to double concentration	$Aloha_{300}$ evaporated after column to double concentration			
Co-precipiation for $Aloha_{1000}$ and $Aloha_{300}$	2.5 µg	0.6 to 1.6 µg	2.5 µg	1.4 µg		1.8 µg

Table A1: Detailed Overview of chemical preparation and measurement methods (2/5; Nu Plasma)

Group	4	5	6	7	9	10
Mass spectrometer	Nu plasma (1700) HR-MC-ICP-MS	Nu plasma (II) MC-ICP-MS	Nu plasma (II) MC-ICP-MS	Nu plasma (1700) HR-MC-ICP-MS	Nu plasma (II) MC-ICP-MS	Nu plasma (II) MC-ICP-MS
Sample introduction	Desolvator DSN-100; PFA nebulizer; ~75µL/min uptake rate	wet plasma glass nebulizer ~100µL/min uptake rate	Desolvator Cetac Aridus II PFA nebulizer ~70µL/min uptake rate	Desolvator Cetac Aridus II PFA nebulizer, ~100µL/min uptake rate	Desolvation Nebulizer System PFA nebulizer ~80µL/min uptake rate	DeSolvation Nebulizer (DSN-100) PFA nebulizer ~70 µL/min uptake rate
Cones	common Ni cones	common Ni cones	common Ni cones	common Ni cones	common Ni cones	common Ni cones
Torch	semi-demountable quartz torch	glass	glass	glass	glass	glass
	alumina injector					
Measurement mode	high resolution	medium resolution; m/Δm 4000-7000	medium resolution	high resolution	medium resolution	medium resolution
Standard-Sample-Bracketing	yes	yes	yes	yes	yes	yes
	smp. repeated 5 times	smp. repeated 3 times	smp. repeated 4-5 times	smp. repeated 3 times	smp. repeated 4~5 times	smp. repeated 3 times
	1 block, 36 cycles of 5sec each	2 blocks, 20 cycles	1 block, 60 cycles	1 block, 25 cycles , 10 sec	1 block, 20 cycles	4 block, 15 cycles
Measurement intensity (^{28}Si)	6-7 V	2-3.5 V/ppm	4 V	9 V for 0.35 ppm Si	6 V	5.5 V/ppm
Blanks (^{28}Si)	10 to 30 mV	10-30 mV	10 to 30 mV	40-100 mV, measured by OPZ	50 to 80 mV	16 to 36 mV

Table A1: Detailed Overview of chemical preparation and measurement methods (3/5; Neptune)

Group	**1**	**2**	**3**	**11**
Sample Vol. ($Aloha_{300}$)	-	50ml	-	8ml
Sample Vol. ($Aloha_{1000}$)	10ml	10ml	100mL	1ml
Precipitation Method	MAGIC	MAGIC	Triethylamine silicomolybdate	MAGIC
	Sodium Hydroxide	Sodium Hydroxide	Sodium Hydroxide	Ammonium Hydroxid
Column Chemistry	Cation Exchange Resin	Cation Exchange Resin	Anion Exchange Resin	Cation Exchange Resin (Dowex 50W-X8)
	(AG50W-X12, 200-400 mesh)	(AG50W-X12, 200-400 mesh)	(AG1-X8)	
Amount Si (µg) introduced in the machine	0.6 ppm	7 µg	1.2 µg	2.5 µg
Mg Doping (yes/no)	yes	yes	Yes	no
Extras	treatment with H_2O_2/UV light	sulfate doping; anion concentration checked; $Aloha_{300}$ evaporated after column to double concentration	Combustion of precipitate in platinum crucibles Dissolution of purified SiO_2 in HF	no
Co-precipitation for $Aloha_{1000}$ and $Aloha_{300}$	yes/yes	yes/yes	yes/yes	yes/yes

Table A1: Detailed Overview of chemical preparation and measurement methods (4/5; Neptune)

Group	**1**	**2**	**3**	**11**
Mass spec	Neptune Plus MC-ICP-MS	Neptune Plus MC-ICP-MS	Thermo Scientific Neptune MC-ICP-MS	Neptune MC-ICP-MS
	(Thermo-Fisher, Germany)	(Thermo-Fisher, Germany)		
Sample introduction	Wet Plasma; Quartz spray chamber; PFA nebulizer; ~70µL/min uptake rate	Desolvator APEX (ESI); PFA nebulizer; 100 µL/min uptake rate	Desolvator Apex (ESI); PFA nebulizer; 100µL/min uptake rate	Apex-IR; PFA nebulizer; ~100µL/min; uptake rate
Cones	H-skimmer, Jet-sampler (Ni cones)	Nickel X-Skimmer cone	common Ni cones	Standard sampling cone
		Standard Ni-Sample cone		X skimmer cone
Torch	glass	Quartz + alumina injector	glass	glass
Measurement mode	medium resolution	medium resolution	medium resolution	medium resolution
	standard-sample bracketing	standard-sample bracketing	standard-sample bracketing	standard-sample bracketing
	smp repeated 3 times	smp repeated 2-3 times	>3 replicates	smp repeated 3 times
	1 block, 30 cycles	3 blocks, 20 cycles per block	1 block, 25 cycles	1 block, 30 cycles, 8s integration time
Measurement intensity (^{28}Si)	8 V	6 V	12 V	2.5 to 3 V
Blanks (^{28}Si)	20 to 30 mV	10 to 50 mV	10 to 30 mV	10 to 20 mV

Table A1: Detailed Overview of chemical preparation and measurement methods (5/5; IRMS)

Group	**8**
Sample Vol. ($Aloha_{300}$)	2000ml
Sample Vol. ($Aloha_{1000}$)	200ml
Precipitation Method	TEA Moly
Column Chemistry	no column chemistry
Mg Doping (yes/no)	no
Extras	Combustion of precipitate in platinum crucibles
	Dissolution of purified SiO2 in HF, precipitation as Cs2SiF6
Instrument Setting	
Mass spec	Finnigan Mat 252 IRMS
Introduction	modified Kiel III inlet system
	98% Sulfuric Acid decomposition of Cs2SiF6 to SiF4
Cones	
Torch	
Measurement mode	standard-sample bracketing
	>3 replicates
	1 block, 20 cycles, 8s integration time
Amount Si introduced in the machine	6μmol
Measurement intensity ($^{28}SiF_3^+$)	2V to 8V
Blanks ($^{28}SiF_3^+$)	No blank

Table A2: Measurements of $\delta^{30}Si(OH)_4$ and $^{29}Si(OH)_4$ by each laboratory group for $ALOHA_{1000}$. The means of analytical replicates, $\delta^{30}Si$ and $\delta^{29}Si$, and associated 2 sigma standard deviations where analytical replicates are defined as replicate analyses from the same chemical preparation. Averages across chemical preparations within a laboratory group are given by $\delta^{30}Si\_mean$ and $\delta^{29}Si\_mean$ with associated 2 sigma standard deviations, 2sd_mean. N and n denote the total number of chemical preparations and analytical replicates for each laboratory group, respectively. NaN indicates data not available.

Group	**$\delta^{30}Si$**	**2 s.d.**	**$\delta^{29}Si$**	**2 s.d.**	**$^{29/30}Si$**	**n**	**$\delta^{30}Si$ mean**	**2 s.d. mean**	**$\delta^{29}Si$ mean**	**2 s.d. mean**	**N**	**n**
Aloha 1000m	**[‰]**	**[‰]**	**[‰]**	**[‰]**	**[‰]**	**analyt. replicate**	**[‰]**	**[‰]**	**[‰]**	**[‰]**		
1	1.15	0.02	0.68	0.07	0.59	**1**	1.10	0.07	0.63	0.07	**4**	**4**
	1.07	0.05	0.62	0.04	0.58	**1**						
	1.09	0.08	0.61	0.03	0.56	**1**						
	1.08	0.07	0.61	0.06	0.56	**1**						
2	1.15	0.01	0.56	0.04	0.49	**3**	1.10	0.07	0.56	0.02	**5**	**15**
	1.09	0.04	0.55	0.01	0.51	**2**						
	1.07	0.01	0.57	0.05	0.53	**3**						
	1.07	0.06	0.55	0.03	0.51	**4**						
	1.12	0.06	0.57	0.04	0.51	**3**						
3	1.14	0.08	0.59	0.05	0.52	**3**	1.16	0.16	0.59	0.09	**3**	**9**
	1.10	0.00	0.55	0.06	0.50	**3**						
	1.25	0.09	0.64	0.08	0.51	**3**						
4	1.28	0.13	0.66	0.08	0.52	**6**	1.17	0.20	0.62	0.10	**3**	**12**
	1.17	0.07	0.62	0.09	0.53	**3**						
	1.08	0.13	0.56	0.07	0.52	**3**						
5	1.19	0.19	0.66	0.10	0.55	**5**	1.23	0.08	0.64	0.04	**4**	**15**
	1.20	0.32	0.62	0.07	0.52	**3**						
	1.27	0.08	0.66	0.04	0.52	**3**						
	1.25	0.13	0.62	0.14	0.50	**4**						
6	1.27	0.10	0.68	0.07	0.53	**1**	1.26	0.12	0.68	0.09	**5**	**5**
	1.28	0.11	0.68	0.13	0.53	**1**						
	1.18	0.23	0.67	0.16	0.57	**1**						
	1.22	0.22	0.62	0.07	0.51	**1**						
	1.33	0.37	0.74	0.12	0.56	**1**						
7	1.29	0.08	0.70	0.04	0.54	**8**	1.25	0.07	0.65	0.07	**6**	**31**
	1.28	0.08	0.62	0.11	0.48	**9**						
	1.27	0.09	0.66	0.04	0.52	**5**						
	1.25	0.10	0.65	0.06	0.52	**3**						
	1.22	0.19	0.66	0.23	0.54	**3**						
	1.20	0.17	0.60	0.19	0.50	**3**						
8	1.27	0.11	0.64	0.06	0.51	**12**	1.29	0.04	0.66	0.02	**4**	**25**
	1.29	0.10	0.66	0.05	0.51	**6**						
	1.27	0.02	0.65	0.01	0.51	**2**						
	1.31	0.11	0.67	0.06	0.51	**5**						

Table A2 continued: Measurements of $\delta^{30}Si(OH)_4$ and $^{29}Si(OH)_4$ by each laboratory group for $ALOHA_{1000}$.

Group	**δ^{30}Si**	**2 s.d.**	**δ^{29}Si**	**2 s.d.**	**$^{29/30}$Si**	**n**	**δ^{30}Si mean**	**2 s.d. mean**	**δ^{29}Si mean**	**2 s.d. mean**	**N**	**n**
Aloha 1000m	**[‰]**	**[‰]**	**[‰]**	**[‰]**	**[‰]**	**analyt. replicate**	**[‰]**	**[‰]**	**[‰]**	**[‰]**		
9	1.32	0.08	0.69	0.01	0.52	**2**	1.31	0.15	0.68	0.09	**10**	**20**
	1.35	0.07	0.74	0.13	0.55	**2**						
	1.42	0.16	0.69	0.14	0.49	**2**						
	1.30	0.11	0.67	0.04	0.51	**2**						
	1.35	0.21	0.70	0.06	0.52	**2**						
	1.33	0.01	0.72	0.07	0.54	**2**						
	1.15	0.07	0.63	0.03	0.55	**2**						
	1.24	0.07	0.64	0.24	0.51	**2**						
	1.34	0.11	0.60	0.11	0.45	**2**						
	1.31	0.14	0.73	0.10	0.55	**2**						
10	1.39	0.09	0.70	0.04	0.50	**3**	1.45	0.17	0.76	0.16	**3**	**9**
	1.55	0.18	0.85	0.08	0.55	**3**						
	1.41	0.12	0.74	0.07	0.52	**3**						
11	1.26	0.11	0.62	0.08	0.50	**9**	1.27	0.05	0.65	0.03	**8**	**72**
	1.25	0.14	0.66	0.07	0.52	**9**						
	1.23	0.16	0.64	0.08	0.52	**9**						
	1.27	0.10	0.65	0.12	0.51	**9**						
	1.30	0.11	0.67	0.08	0.52	**9**						
	1.28	0.23	0.66	0.09	0.51	**9**						
	1.30	0.16	0.66	0.09	0.50	**9**						
	1.28	0.16	0.66	0.10	0.52	**9**						

Table A2: Measurements of $\delta^{30}Si(OH)_4$ and $^{29}Si(OH)_4$ by each laboratory group for $ALOHA_{300}$. The means of analytical replicates, $\delta^{30}Si$ and $\delta^{29}Si$, and associated 2 sigma standard deviations where analytical replicates are defined as replicate analyses from the same chemical preparation. Averages across chemical preparations within a laboratory group are given by $\delta^{30}Si$_mean and $\delta^{29}Si$_mean with associated 2 sigma standard deviations, 2sd_mean. N and n denote the total number of chemical preparations and analytical replicates for each laboratory group, respectively. NaN indicates data not available.

Group	**$\delta^{30}Si$**	**2 s.d.**	**$\delta^{29}Si$**	**2 s.d.**	**$^{29/30}Si$**	**n**	**$\delta^{30}Si$ mean**	**2 s.d. mean**	**$\delta^{29}Si$ mean**	**2 s.d. mean**	**N**	**n**
Aloha 300 m	**[‰]**	**[‰]**	**[‰]**	**[‰]**	**[‰]**	**analyt. replicate**	**[‰]**	**[‰]**	**[‰]**	**[‰]**		
2	1.75	0.02	0.83	0.03	0.48	**2**	1.66	0.10	0.84	0.05	**6**	**12**
	1.64	0.01	0.87	0.05	0.53	**2**						
	1.62	0.04	0.86	0.01	0.53	**2**						
	1.65	0.02	0.81	0.05	0.49	**2**						
	1.67	0.03	0.81	0.02	0.49	**1**						
	1.63	0.06	0.85	0.04	0.52	**3**						
4	1.56	0.06	0.87	0.09	0.55	**3**	1.64	0.13	0.87	0.05	**4**	**12**
	1.60	0.12	0.83	0.02	0.52	**3**						
	1.66	0.12	0.86	0.01	0.52	**3**						
	1.71	0.09	0.90	0.03	0.53	**3**						
5	1.52	0.17	0.76	0.07	0.50	**4**	1.51	0.12	0.80	0.08	**3**	**11**
	1.56	0.18	0.84	0.14	0.53	**4**						
	1.45	0.08	0.81	0.05	0.56	**3**						
6	1.95	0.37	0.98	0.19	0.50	**1**	1.78	0.18	0.89	0.18	**6**	**6**
	1.76	0.27	0.90	0.17	0.51	**1**						
	1.76	0.30	0.86	0.19	0.49	**1**						
	1.75	0.07	0.74	0.16	0.42	**1**						
	1.68	0.37	0.98	0.12	0.58	**1**						
	1.81	0.38	0.91	0.22	0.50	**1**						
7	1.92	0.13	0.98	0.05	0.51	**2**	1.92	0.08	1.02	0.12	**5**	**14**
	1.97	0.02	1.05	0.11	0.53	**3**						
	1.95	0.08	1.07	0.01	0.55	**3**						
	1.87	0.30	0.94	0.32	0.50	**3**						
	1.89	0.07	1.07	0.08	0.57	**3**						
8	1.51	0.05	0.77	0.05	0.51	**3**	1.46	0.17	0.75	0.09	**3**	**10**
	1.52	0.04	0.77	0.02	0.51	**1**						
	1.36	0.09	0.69	0.04	0.51	**6**						
9	1.90	0.01	0.95	0.06	0.50	**2**	1.94	0.12	0.99	0.08	**8**	**16**
	2.05	0.16	1.06	0.08	0.52	**2**						
	1.90	0.57	0.98	0.21	0.51	**2**						
	1.94	0.01	0.94	0.10	0.48	**2**						
	2.02	0.42	1.04	0.11	0.51	**2**						
	1.91	0.10	1.00	0.24	0.52	**2**						
	1.89	0.27	0.99	0.14	0.53	**2**						
	1.95	0.27	1.01	0.10	0.52	**2**						

Table A2 continued: Measurements of $\delta^{30}Si(OH)_4$ and $^{29}Si(OH)_4$ by each laboratory group for $ALOHA_{300}$.

Group **Aloha 300 m**	**δ^{30}Si**	**2 s.d.**	**δ^{29}Si**	**2 s.d.**	**$^{29/30}$Si**	**n**	**δ^{30}Si mean**	**2 s.d. mean**	**δ^{29}Si mean**	**2 s.d. mean**	**N**	**n**
	[‰]	**[‰]**	**[‰]**	**[‰]**	**[‰]**	**analyt. replicate**	**[‰]**	**[‰]**	**[‰]**	**[‰]**		
10	1.52	0.04	0.77	0.02	0.51	**3**	1.53	0.17	0.79	0.06	**3**	**9**
	1.45	0.05	0.77	0.02	0.53	**3**						
	1.61	0.07	0.82	0.06	0.51	**3**						
11	1.61	naN	0.88	naN	0.55	**1**	1.69	0.24	0.85	0.17	**8**	**8**
	1.82	naN	0.97	naN	0.54	**1**						
	1.73	naN	0.90	naN	0.52	**1**						
	1.52	naN	0.71	naN	0.46	**1**						
	1.60	naN	0.77	naN	0.48	**1**						
	1.76	naN	0.91	naN	0.52	**1**						
	1.86	naN	0.85	naN	0.46	**1**						
	1.61	naN	0.80	naN	0.50	**1**						

Table A3: Summary of mean Si isotope values ($\delta^{30}Si$, $\delta^{29}Si$), the associated 2σ analytical uncertainty (2 s. d.) and the number of measurements (n) obtained by each laboratory group for the secondary standards Big Batch and Diatomite. The overall mean and the uncertainty about the mean (2 s. d.) as well as the median and the interquartile deviation (IQD) for all groups are given at the bottom of the table. NaN indicates data not available.

Group	Big Batch					Diatomite				
	$\delta^{30}Si$	2 s.d.	$\delta^{29}Si$	2 s.d.	n	$\delta^{30}Si$	2 s.d.	$\delta^{29}Si$	2 s.d.	n
1	-10.61	0.08	-5.42	0.07	18	1.25	0.11	0.64	0.09	15
2	NaN	NaN	NaN	NaN	NaN	1.26	0.14	0.66	0.12	14
3	-10.48	0.34	NaN	NaN	3	NaN	NaN	NaN	NaN	NaN
4	NaN	NaN	NaN	NaN	NaN	1.25	0.13	NaN	NaN	19
5	-10.67	0.16	-5.43	0.10	5	1.23	0.05	0.63	0.04	4
6	-10.64	0.22	-5.43	0.10	34	NaN	NaN	NaN	NaN	NaN
7	-10.50	0.08	-5.36	0.06	3	NaN	NaN	NaN	NaN	NaN
8	-10.51	0.23	-5.35	0.11	25	1.27	0.16	0.66	0.07	5
9	-10.48	0.08	NaN	NaN	2	NaN	NaN	NaN	NaN	NaN
10	NaN	NaN	NaN	NaN	NaN	NaN	NaN	NaN	NaN	NaN
11	NaN	NaN	NaN	NaN	NaN	NaN	NaN	NaN	NaN	NaN
Mean	**-10.56**		**-5.40**			**1.25**		**0.65**		
2 s.d.	**0.16**		**0.08**			**0.03**		**0.03**		
Median	**-10.51**		**-5.42**			**1.25**		**0.65**		
IQD	**0.07**		**0.04**			**0.01**		**0.01**		

Table A4: Statistical Analysis of Differences in differences in $\delta^{30}Si(OH)_4$ among groups using Neptune spectrometers. Groups not connected by same letter are significantly different.

$ALOHA_{1000}$					
	Tukey		False Discovery Rate		Mean $\delta^{30}Si(OH)_4$
Group	Column A	Column B	Column A	Column B	
11	A		A		1.27
2		B	A	B	1.16
3		B		B	1.10
1		B		B	1.10
$ALOHA_{300}$					
	Tukey				
Group	Column A	Column B			
11	A				1.69
2	A				1.66

Table A5: Statistical Analysis of Differences in differences in $\delta^{30}Si(OH)_4$ among groups using Nu Plasma mass spectrometers. Groups not connected by same letter are significantly different.

$ALOHA_{1000}$				
	Tukey			Mean $\delta^{30}Si(OH)_4$
Group	Column A	Column B	Column C	
10	A			1.45
9		B		1.31
6		B	C	1.26
7		B	C	1.25
5		B	C	1.23
4			C	1.18
$ALOHA_{300}$				
9	A			1.94
7	A			1.92
6		B		1.78
4			C	1.64
10			C	1.53
5			C	1.51

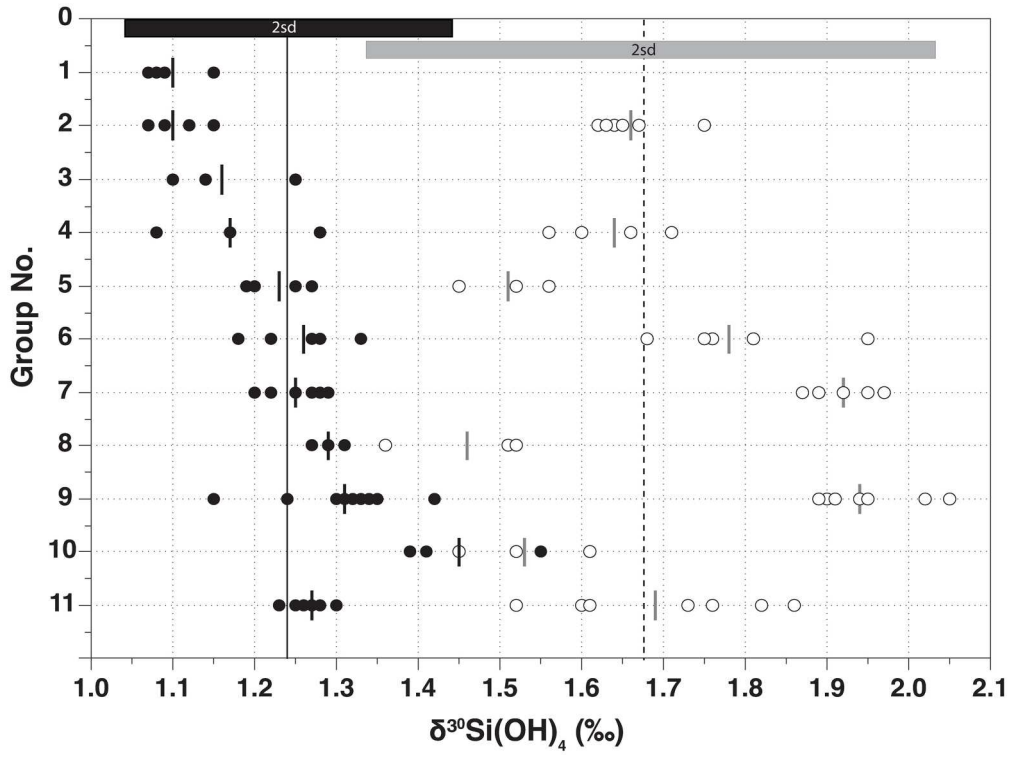

Figure 1. $\delta^{30}Si(OH)_4$ results from all groups for $ALOHA_{300}$ (open circles) and $ALOHA_{1000}$ (filled circles). The long black vertical solid line indicates the mean value of all measurements for $ALOHA_{1000}$ and the long dashed line that for $ALOHA_{300}$. The data points represent the individual $\delta^{30}Si(OH)_4$ values from Table A2. Short vertical solid lines are the means obtained by individual laboratories for the two samples. Uncertainty in the mean for all measurements for each sample (2 s. d.) is indicated by the horizontal bars at the top of the figure.

Fig. 1
188x141mm (300 x 300 DPI)

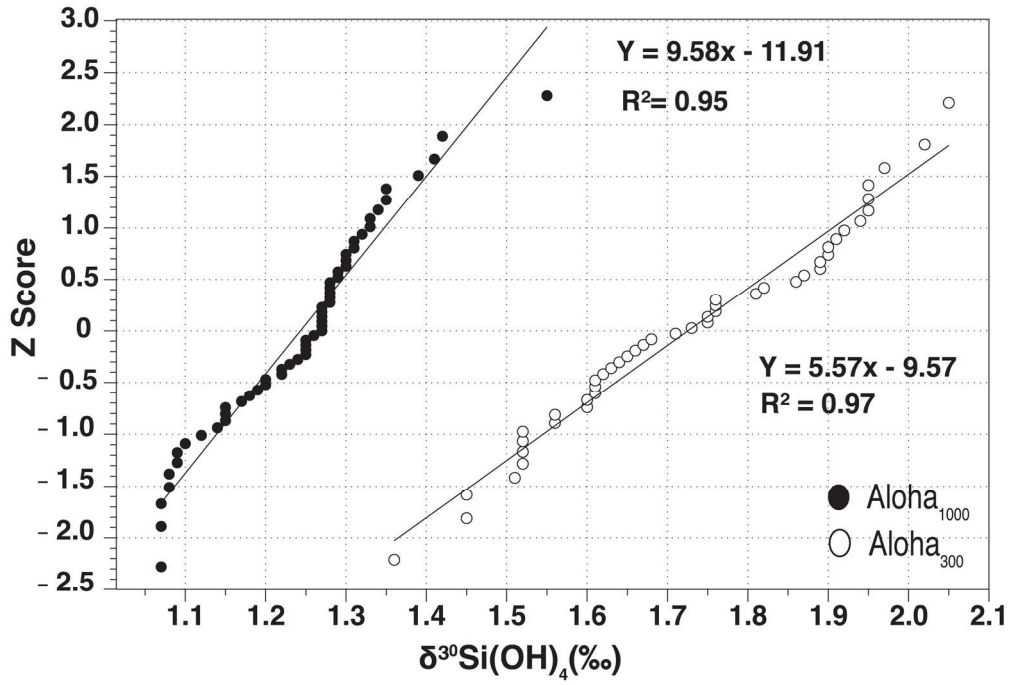

Figure 2. Z scores as a function of $\delta^{30}Si(OH)_4$ for $ALOHA_{300}$ (open circles) and $ALOHA_{1000}$ (filled circles).
Fig. 2
155x106mm (300 x 300 DPI)

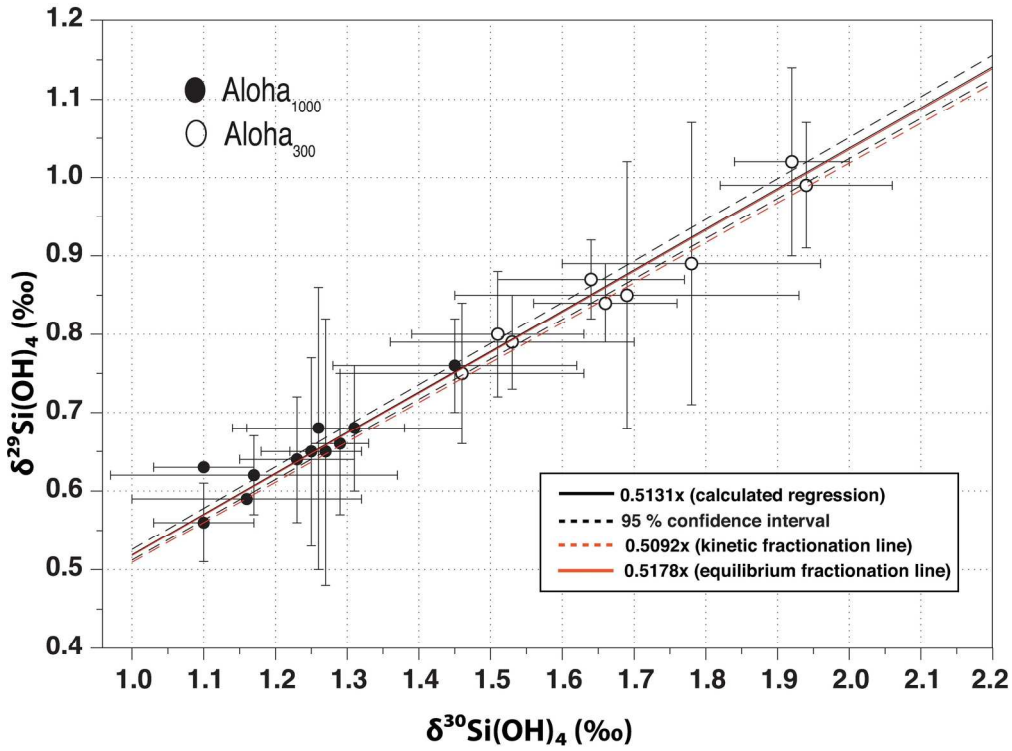

Figure 3. Plot of $\delta^{30}Si(OH)_4$ versus $\delta^{29}Si(OH)_4$ for ALOHA300 (open circle) and $ALOHA_{1000}$ (filled circle; error bars are 2 s. d.). Solid line is the result of least-squares linear regression with a slope of 0.5188 ± 0.0184 (s.e., R^2 = 0.98). The lower and upper 95 % confidence intervals are given as dashed black lines. The kinetic fractionation line has a slope of 0.5092 (intercept of zero) for Si (dashed red line) and the equilibrium fractionation line has a slope of 0.5178 (intercept of zero) for Si (solid red line). Regression line obtained by analysis using reduced major axis model II regression yields a slope of 0.5131 ± 0.0040 (s.e., R^2 = 0.98; not displayed in the figure).

Fig. 3

176x131mm (300 x 300 DPI)

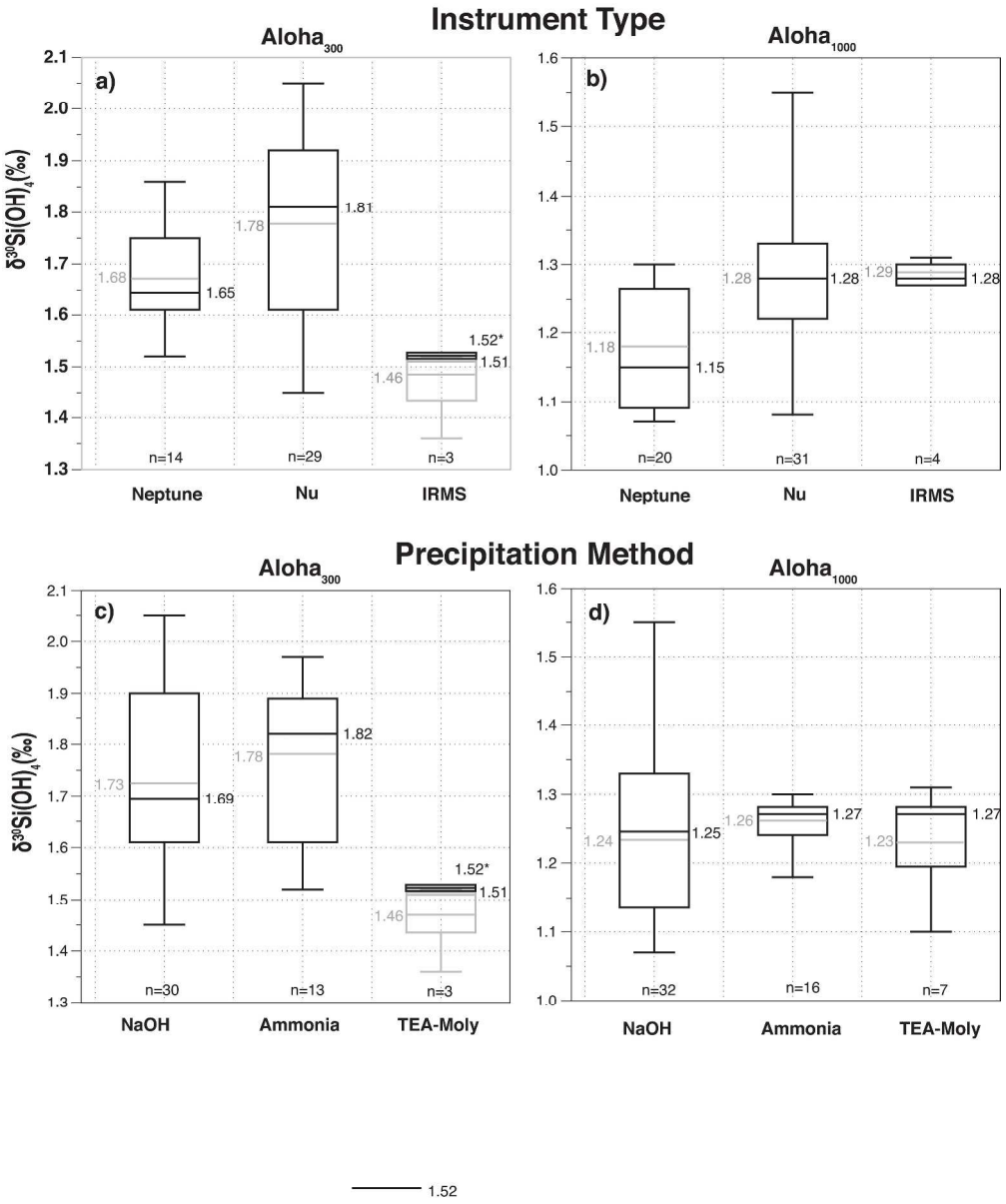

Figure 4. Boxplots showing $\delta^{30}Si(OH)_4$ data sorted by different mass spectrometer types for a) $ALOHA_{300}$ and for b) $ALOHA_{1000}$. Data sorted by different precipitation methods for c) $ALOHA_{300}$ and d) $ALOHA_{1000}$. On the boxplots the median values (black) and the mean values (grey) are displayed. For $ALOHA_{300}$ a) and c) show data for IRMS and TEA-Moly with (grey boxplot) and without outlier (black boxplot). Here, the mean value (which equals the median) is indicated by a superscript star. The value next to each boxplot indicates the median (black) and the mean (grey), respectively. The number of included data points (n) is given below each boxplot. Raw data are presented in Table 3

Fig. 4
334x402mm (300 x 300 DPI)